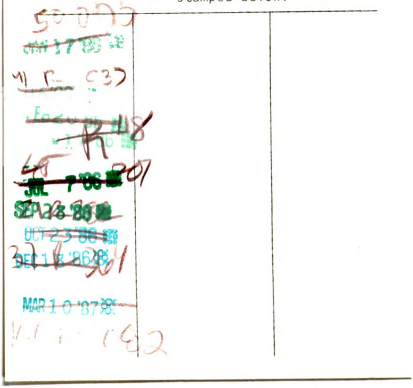

MARTENSITIC TRANSFORMATION OF Ni_3Sn ALLOY

By

Soon- Nam Chang

A THESIS

Submitted to
Michigan State University
in partial fulfillment of the requirements
for the degree of

MASTER OF SCIENCE

Department of Metallurgy, Mechanics
and Materials Science

1982

ABSTRACT

MARTENSITIC TRANSFORMATION OF Ni_3Sn ALLOY

By

Soon- Nam Chang

The Martensite of Ni_3Sn has been investigated crystallographically by means of transmission electron diffraction as well as optical microscopy. The crystal structure of the martensite was identified as the β-Cu_3Ti (2H)-type orthorhombic structure. It was found that the high temperature, parent phase of Ni_3Sn was impossible to retain at room temperature. For such a case or for another case where small amounts of parent phases were only retained, a new method was proposed to determine the orientation of the habit plane of martensite plates and the orientation of the specimen surface before martensitic transformation. This method was applied to Ni_3Sn martensite and {122} plane was determined as the habit plane of Ni_3Sn. The determined habit plane was compared with the habit plane predicted by the strain energy minimization criterion.

ACKNOWLEDGEMENTS

The author would like to express his deepest appreciation and gratitude his major professors Dr. H-r. Pak and Dr. M. Kato for their advice and guidence in both areas of research work and writing of his thesis.

Dr. K. Mukherjee was also very helpful during this investigation along with Mr. D. Chung, and I wish to extend my appreciation to them also.

A special thanks goes to his family for their patience and encouragement during his study.

TABLE OF CONTENTS

TABLE OF CONTENTS -- continued

LIST OF TABLES

LIST OF FIGURES

LIST OF FIGURES--continued

LIST OF FIGURES--continued

FIGURE Page

1 INTRODUCTION

The name martensite was originally given to the product of the hardening reaction in rapidly cooled steels, but its use has been extended to similar changes in other alloy systems. The definition of a martensitic transformation is a transformation associated with a lattice-distortive, virtually diffusionless structual change having a dominant deviatoric (shear) component.

Any martensite formed by such diffusionless, shear-type atomic motion is mostly embedded in an untransformed phase, so-called parent phase, and bound on a specific plane of the parent phase. This specific plane is called the habit plane and is explained phenomenologically as a lattice invariant plane. The habit plane and orientation relationships between the parent and martensite phases are important in understanding the martensitic transformation from a crystallographic aspect. Therefore, many works on martensitic transformation have been involved in abtaining such crystallographic informations.

In some cases, however, parent phases can not be retained at room temperature or if any, small amounts of parent phases can be retained. Thus, it is difficult to get crystallographic relationships between the parent and martensite phases.

This research is mainly aimed to determine the orientation of habit planes in cases where no parent phase is retained at room temperature. For this purpose a new method was proposed. Ni_3Sn alloy was employed to apply this method because in this alloy it is theoretically impossible to retain the parent phase. The

determined orientation was compared with the orientation of the habit plane predicted by a phenomenological theory based on the elastic strain energy minimization criterion. The crystal structure and internal structures of the martensite of Ni_3Sn was examined by means of transmission electron diffraction as well as microscopy so that the phenomenological theory could be applied.

2 CRYSTALLOGRAPHY OF Ni_3Sn

2.1 Phase Stability of Ni_3Sn Phases

Figure 2.1 is a phase diagram of Ni-Sn binary alloy [1], and Figure 2.2 shows the detailed phase diagram of Ni_3Sn compound [2]. As can be seen in these figures, Ni_3Sn has a phase transition at around 950°C. The existence of the phase transition was found by Heumann [3] through DTA measurements and this phase transition was attributed to a disorder-order transition from disordered hcp to Mg_3Cd (DO_{19})-type ordered hcp structure. Schubert et al [4], however, investigated a crystal structure X-ray technique, and found that the crystal structure was not the disordered hcp but Fe_3Al (DO_3) -type ordered bcc structure.

Recently, Pak and co-workers [5] investigated the relation between the high-temperature phase with the DO_3-type structure and the low-temperature phase with the DO_{19}-type structure in detail, and found that the DO_{19}-type structure being stable at room temperature was transformed massively from the DO_3-type structure when quenched slowly. It was also found that when quenched rapidly the DO_3-type structure was transformed martensitically into the β-Cu_3Ti-type (2H) ordered orthorhombic structure.

Figure 2.3 shows the unit cell of DO_3-type structure for the high temperature phase of Ni_3Sn alloy and Table 2.1 shows the lattice parameter of the DO_3 type structure.

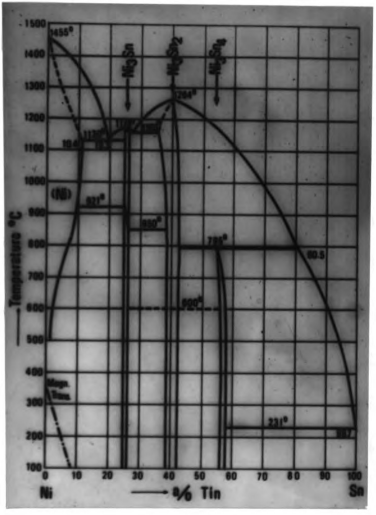

Figure 2.1 Ni - Sn phase diagram.

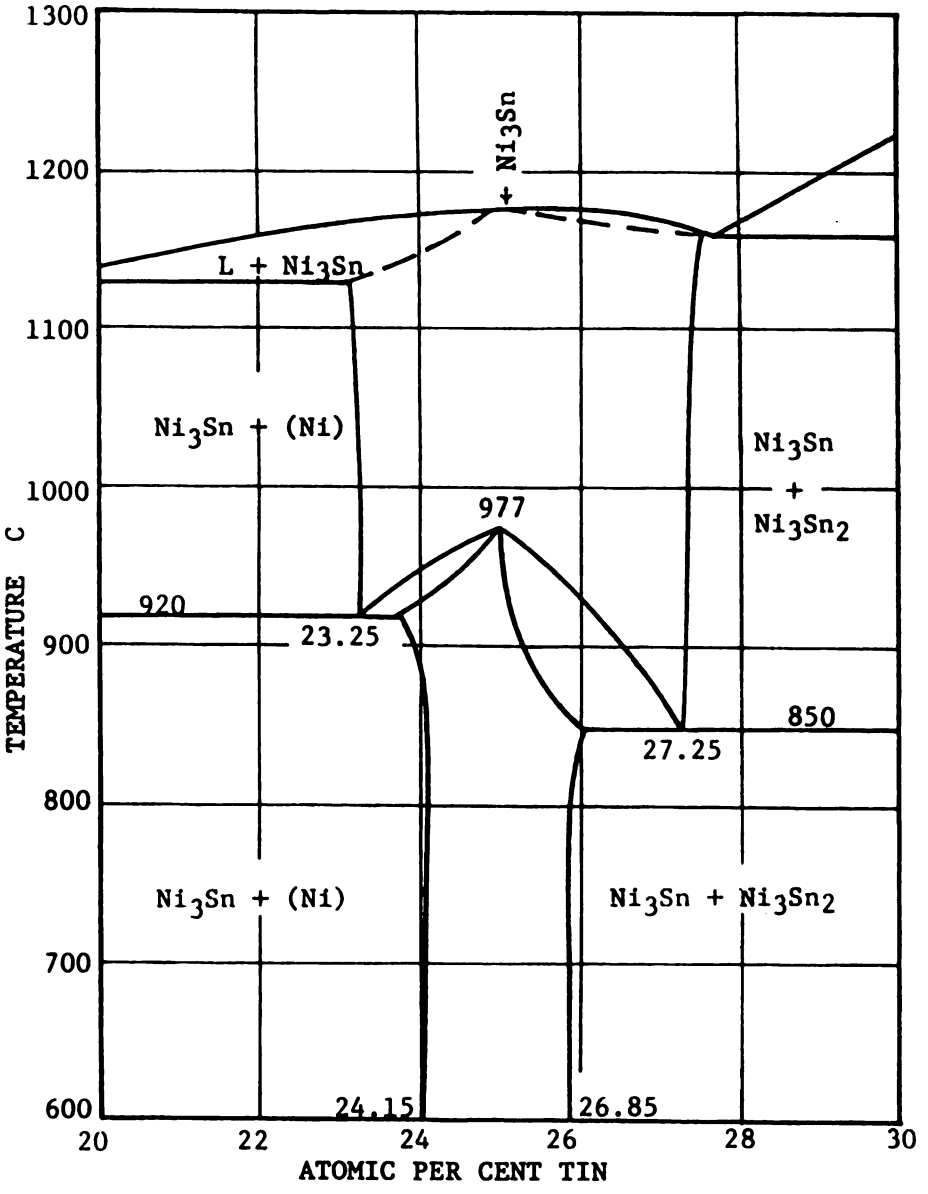

Figure 2.2 The detailed phase diagram of Ni_3Sn compound.

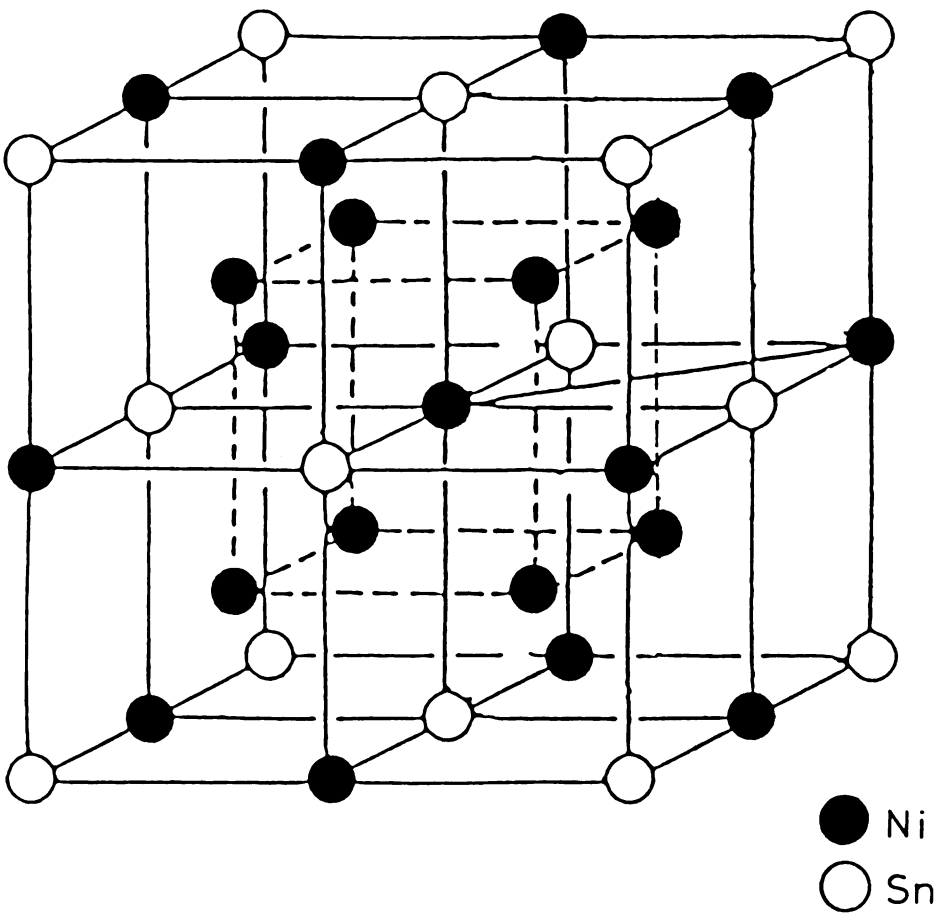

Figure 2.3 The unit cell of DO_3-type structure.

2.2 Crystal Structure of Ni_3Sn Martensite Phase

As mentioned in the previous section, Pak and co-workers [5] determined the crystal structure of the martensite phase as the β-Cu_3Ti (2H)-type structure by means of X-ray diffraction. The unit cell of the martensite phase is drawn in Figure 2.4 and atomic positions of Sn and Ni atoms in the unit cell are listed below

Sn	(0 0 0) (2/3 1/2 1/2)
Ni	(0 1/2 0) (1/2 1/4 0) (1/2 3/4 0)
	(2/3 0 1/2) (1/6 3/4 1/2) (1/6 1/4 1/2).

Since the crystal structure of the martensite was determined only by means of X-ray diffraction, the structural determination of the martensite was carried out by means of transmission electron diffraction in order to make sure whether the martensite has the Cu_3Ti-type structure or not. This will be shown in the following section. Table 2.2 shows the lattice parameters of this structure.

2.3 Crystal Structure Determination of the Ni_3Sn Martensite

For the convenience of the structure determination, the crystal structure of the martensite was assumed to be the β-Cu_3Ti-type structure. According to the diffraction theory, the structure factor of the crystal is expressed as,

$$F_g = \sum_i f_i \exp(2\pi i \bar{g} \cdot \bar{r}_i) ,$$

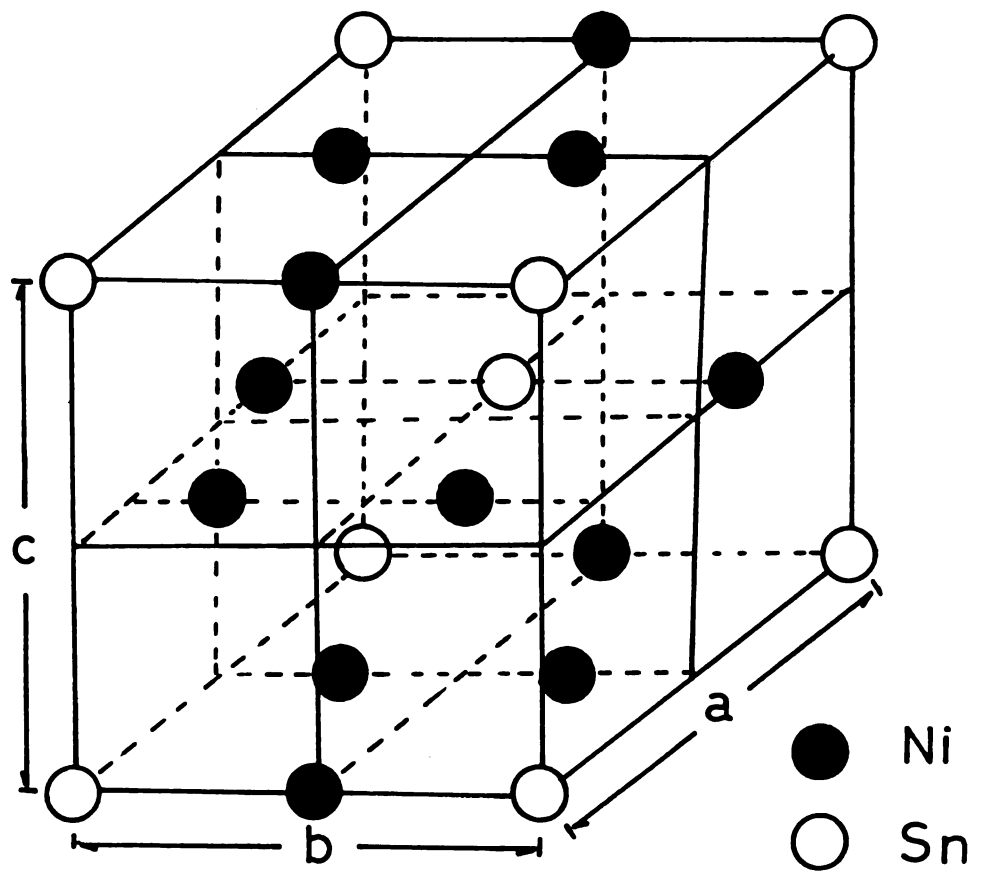

Figure 2.4 The unit cell of β-Cu_3Ti-type structure.

Table 2.1 Lattice parameters of DO_3-type structure.

lattice parameter (A)	remarks	author
6.091	Ni-Sn at 950 C	Schubert
5.9580	Cu-Al	Tarora
5.80 ± .05	Cu-Al-Ni	Duggin & Rachinger
5.836	Cu-Al-Ni	Otsuka & Shimizu
5.8412 ± .0004	Cu-Al-Ni at 21 C	Duggin

Table 2.2 Lattice parameters of β-Cu_3Ti type martensite.

a(A)	b(A)	c(A)	alloy	author
4.41	5.31	4.22	Cu-Al-Ni	Duggin & Rachinger
4.40(±0.5%)	5.33(±0.5%)	4.24(±0.5%)	Cu-Al-Ni	Duggin
4.6011	5.3050	4.3052	Cu-Al	Geninger
4.382	5.356	4.222	Cu-Al-Ni	Otsuka & Shimizu
4.504	5.304	4.277	Ni-Sn	Pak et al

where fi is the atomic scattering factor of the i-th atom and in the real lattice unit cell. The vector $\bar{r}i$ is expressed by

$$\bar{r}i = ui\bar{a} + vi\bar{b} + wi\bar{c}$$

where ui, vi, wi are fractional coordinates of the i-th atom, and $\bar{a}$, $\bar{b}$ and $\bar{c}$ are the translations of the real lattice unit cell.

If $\bar{a}^*$, $\bar{b}^*$ and $\bar{c}^*$ are the translations of the reciprocal lattice unit cell, every reciprocal lattice point can be expressed by the form

$$\bar{g} = h\bar{a}^* + k\bar{b}^* + l\bar{c}^*$$

where h,k and l are intrgers. $\bar{g}$ is normal to the crystal plane with Miller indices hkl. Thus, $\bar{g} \cdot \bar{r}i$ is abtained as

$$\bar{g} \cdot \bar{r}i = hui + kvi + lwi \ .$$

The structure factor for layered structures such as 2H-type structure can be obtained by the simple sum of the structure factor related with each layer. There are one A-atom and three B-atoms on the (001) of the β-Cu_3Ti lattice, the coordinates are 0 0 0 , and 0 1/2 0 , 1/2 1/4 0 , 1/2 3/4 0 , respectively. The cooresponding atoms on the next (001) are all displaced by [2/3 1/2 1/2]. Thus,

$$F_g = F_1 + F_2 \ ,$$
$$F_1 = f_A + f_B \{e^{-2\pi i(h/2 + k/4)} + e^{-2\pi i(h/2 + 3k/4)} + e^{-2\pi i(k/2)}\} \ ,$$

and $$F_2 = F_1 e^{-2\pi i(2h/3 + k/2 + 1/2)} .$$

Here, F_1 is the structure factor on the first (001) plane in unit cell(shown Figures 2.4 and 3.3), F_2 the structure factor on the second (001) plane in unit cell(shown Figures 2.4 and 3.3), f_A the atomic scattering factor for A atom and f_B the atomic scattering factor for B atom. Multiplication by the complex conjugate of F_g will give us the square of the absolute value of the resultant wave amplitute F ; that is,

$$|F|^2 = 4 \{f_A + f_B(2 \cos\pi h \cos\pi k/2 + \cos\pi k)\}^2 \times \cos^2\pi(2/3h + 1/2k + 1/2l).$$

According to diffraction theory, $|F|^2$ is proportional to the intensity I_g of reciprocal lattice points ; that is,

$$I_g \propto |F_g|^2 .$$

$|F|^2$ obtained from the above equation are summarized in Table 2.3 and the resulting reciprocal lattice planes are illustracted in Figure 2.5.

2.3.1 Experimental Procedures

The Ni_3Sn alloy of 24.6 at % Sn was prepared by melting 99.9% pure nickle(supplied by the International Nickle Co.), and 99.999% tin(supplied by K & K Laboratories,INC.), at 1,190°C in 18mm-diameter quartz capsules which was evacuated up to about 1×10^{-5} torr and

Table 2.3 Absolute values $|F|^2$ determined by h,k and l.

h	k	l	$\|F\|^2$
6n 6n±3	4m 4m±2	2q 2q	$4(f_A + 3f_B)^2$
6n±1 6n±2	4m±2 4m	2q±1 2q±1	$3(f_A + 3f_B)^2$
6n±1 6n±2	4m±2 4m	2q 2q	$(f_A + 3f_B)^2$
6n 6n 6n±3 6n±3	4m 4m±2 4m±1 4m	2q±1 2q 2q±1 2q	$4(f_A - f_B)^2$
6n±1 6n±1 6n±2 6n±2	4m 4m±1 4m±1 4m±2	2q±1 2q 2q 2q±1	$3(f_A - f_B)^2$
6n±1 6n±1 6n±2 6n±2	4m 4m±1 4m±1 4m±2	2q 2q±1 2q±1 2q	$(f_A - f_B)^2$
6n(or ±3) 6n(or ±3) 6n(or ±3)	4m 4m±1 4m±2	2q±1 2q 2q±1	0

(m.n.q are integers)

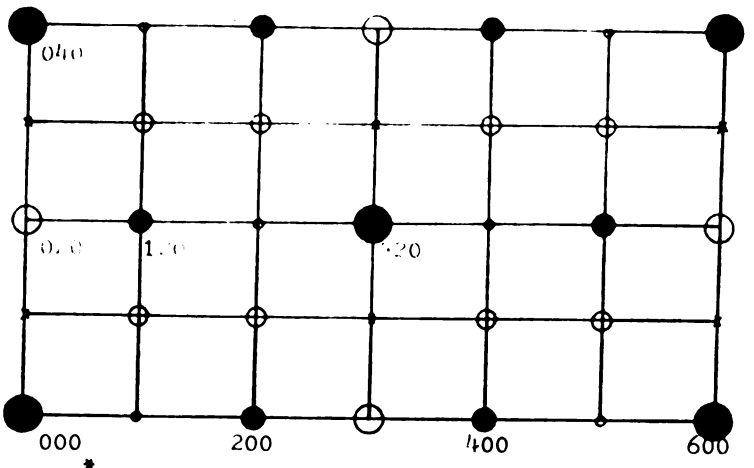

$(001)^*$ passing through 000 point

a = 4.504
b = 5.304
c = 4.277

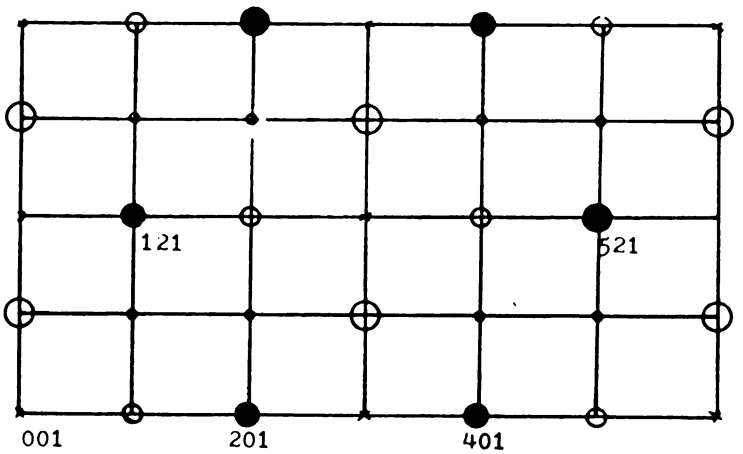

$(001)^*$ passing through 001 point

Fundamental

$2(f_{Sn}+3f_{Ni})=2F$

$\sqrt{3}F$

F

Super-lattice

$2(f_{Sn}-f_{Ni})$

$\sqrt{3}S$

S

Figure 2.5 The reciprocal lattice planes of β-Cu_3Ti type structure

then sealed. The pure nickle rod was cut into small piece after cold rolling and then chemically polished in a 25% HNO_3- 25% H_2SO_4- 37% CH_3COOH- 13% H_2O_2 solution at 60-70°C . Agitation was carried out several times in the molton state in order to mix alloy elements well. The weight losses of the alloy ingot was about 0.03 wt%. The ingot was sealed and evacuated quartz capsule at 1,100°C for 20 hrs to homogenize well.

Then, the ingot was cut by Diamond wafering Blade to the thickness of 1mm, and polished done with 600 grit silicon carbide strip to the thickness, of a 0.7mm to abtain the smooth flat surface. The sheet specimens obtained were then annealed at 1,100°C for 1 hr in evacuated quartz capsules which were crashed when quenched in order that the martensitic transformation took place.

Optical microscope observation was carried out for the confirmation of theoccurence of the martensitic transformation in Ni_3Sn and also for the measurement of possible crystallographical data. Sheet specimens were prepared for this observation by hand-polishing, and etching in a $1Hcl + 2HNO_3 + 6CH_3OH$ solution.

Most of the specimens were thinned down again for transmission electron microscope observation. Jet electropolishing was carried out by using a 25% $HClO_4$ and 75% CH_3CH_2OH solution and then final electrothinning was done at 18 volts at about -65°C by using the same solution. The stainless steel plate was employed as a cathode. Transmission electron microscope observation was carried out by using an electron microscope of Hitachi HV-11A, operated at 100KV.

2.3.2 Experimental Results

Figure 2.6(a) is an optical micrograph of Ni_3Sn, showing fine structures obtained by quenching from 1,190° C. Figure 2.6(b) is an another optical micrograph of Ni_3Sn prepolished before quenching, showing surface relieves. These surface relieves clearly demonstrate that the fine "acicular" structures were formed martensitically. Similar surface relieves of Ni_3Sn were reported by Pak et al [5].

Figure 2.7 is a typical electron micrograph, showing microstructures of the Ni_3Sn martensites, electron diffraction patterns taken from the martensites were analyzed. Some of examples are shown in Figures 2.8,2.9 and 2.10. The crystal structure of the martensite was able to be determined as an ordered orthorhombic structure using the reciprocal lattice constracted. In other words, the structure determined was the same as reported in reference [5]. By using the lattice parameters of the martensite determined by X-ray [5], a = 4.504 A, b = 5.304 A and c = 4.277 A, Figures 2.8 to 2.10 were indexed. Interplanar spacings and interplanar angles calculated using the above mentioned lattice parameter were listed in Appendices A and B.

Figure 2.11(a) is another electron micrograph showing internal structures of the martensite. These internal structures were identified as $(121)_{2H}$ twins from Figure 2.11(b-d),(which were refered from reference (5)). Figure 2.11(b) is an electron diffraction pattern taken from the area of Figure 2.11(a), which obviousely shows the twin relation. Figure 2.11(c) and (d) show dark field images in 201 reflection and 201_T reflection, respectively. It is clear from

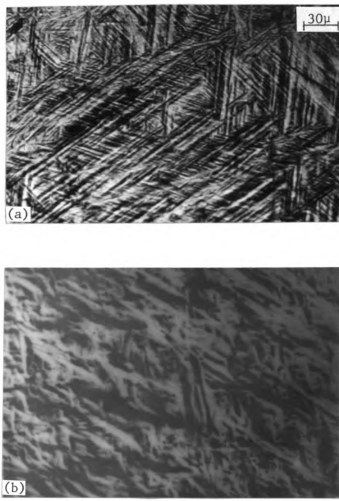

Figure 2.6 (a) Optical micrograph of Ni_3Sn martensite.
(b) Optical micrograph of Ni_3Sn martensite showing surface relieves.

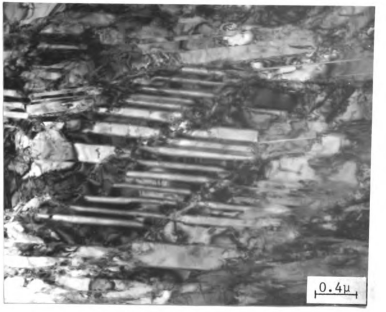

Figure 2.7 Typical transmission electron micrograph showing microstructures of the acicular Ni_3Sn martensite.

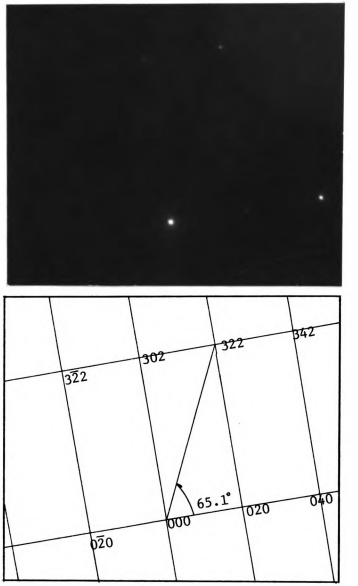

Figure 2.8 Electron diffraction pattern of β-Cu_3Ti-type Ni_3Sn martensite.

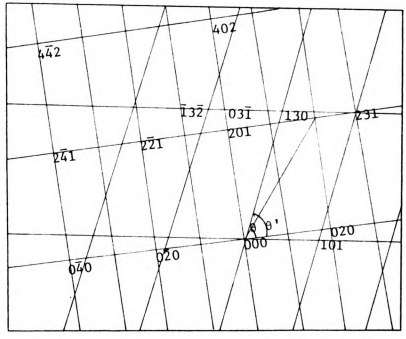

Figure 2.9 Electron diffraction of β-Cu_3Ti-type Ni_3Sn martensite.
θ = 53.1°
θ'= 74°

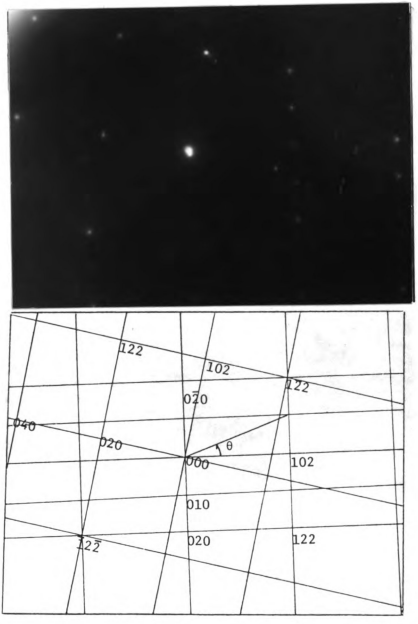

Figure 2.10 Electron diffraction pattern of β-Cu_3Ti-type Ni_3Sn martensite.
$\theta \cong 20°$

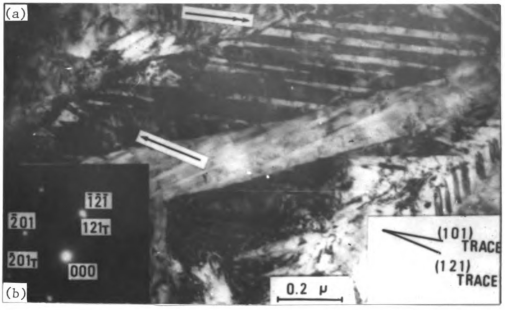

Figure 2.11 (a) Transmission electron micrograph of Ni_3Sn martensite. (b) Electron diffraction pattern taken from the area of (a).

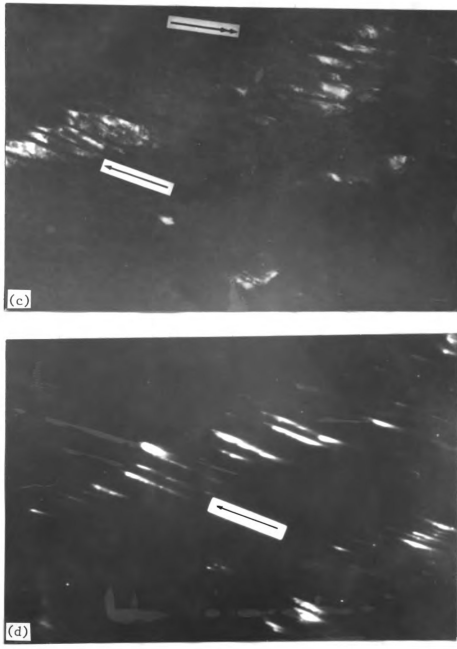

Figure 2.11 (c) (d) Dark field images in 201 and 201_T reflection, respectively.

Figure 2.11(b),(c) and (d) that 201 and 201_T reflections are twin-related to each other. Most of internal bands are $(121)_{2H}$ twins, indicated by arrow↑, while small amounts of bands are parallel to $(101)_{2H}$, which was considered to be another twin plane.

3 HABIT PLANE DETERMINATION OF Ni_3Sn MARTENSITE

3.1 Phenomenological Analysis Based on the Strain Energy Minimization

The martensitic transformations have been discussed by severs1 authors from a viewpoint of the minimization of the elastic strain energy [6-9]. As pointed out by Kato and coworkers [10] recently, the phenomenological analysis based on the elastic strain energy minimization criterion is essentially identical to the phenomenological theories proposed by Wechsler et al [11] and Bowles and Mackenzie [12].

Recently, Mukherjee and Kato [13] applied the elastic strain energy minimization criterion to the crystallography of martensites in Ti alloys and showed that habit planes predicted were in good agreement with those obtained experimentally.

There are some crystallographic similarities of martensites between Ti alloys and Ni_3Sn alloy, such as lattice invariant shear being a twinning shear. Thus, a similar procedure to one employed by Mukherjee and Kato [13] was used in the study to determine the habit plane of the Ni_3Sn martensite.

3.1.1 Lattice Correspondence of DO_3-type Structure and 2H-type Structure

Figure 2.3 illustrates a unit cell of the DO_3-type ordered bcc structure of the parent phase. The atomic positions on (101) plane in the DO_3-type structure are shown in Figure 3.1. As can be seen in Figure 3.1, the DO_3-type structure consists of the AB'AB'

stacking. It is well known that the 2H-type crystal structure (deformed hcp) can be produced from bcc structure by Burgers' mechanism, where the operation of the {112} <11$\bar{1}$> DO_3 shear systems followed by a small volume change results in the $(001)_{2H}$ $(0001)_{hcp}$ plane from the $(101)_{DO_3}$ plane. In addition to this operation, a $a/12[10\bar{1}]_{DO_3}$ suffling on every other $(101)_{DO_3}$ plane is necessary to create the 2H structure as shown in Figure 2.4. To understand this suffling assiciated with the martensitic transformation, atomic positions of the 2H-type structure are illustrated in Figure 3.2. Considering the shearing and suffling operation mentioned above, it can be easily understood that the 2H-type structure is generated from the tetragonal lattice in the DO_3 structure, drawn as a heavy-lined lattice in Figure 3.3.

By using existing lattice parameters of the parent DO_3-phase and martensite phase, the lattice variant strain(Bain strain) can be calculated. The existing lattice parameter of the parent phase is $a_{\beta 1}$ = 6.006 A at 25° C [4] and a_{2H} = 4.504 A , b_{2H} = 5.304 A , c_{2H} = 4.277 A [5]. From this values, the Bain strains based on the x'-y-z' coordinate system in Figure 3.3 are obtained as

$$\varepsilon_1 = \sqrt{2}a_{2H} / a_{\beta 1} - 1 = 0.0605$$
$$\varepsilon_2 = b2H / a_{\beta 1} - 1 = -0.1169$$
$$\varepsilon_3 = \sqrt{2}c_{2H} / a_{\beta 1} - 1 = 0.0071 \qquad (3.1)$$

and the volume change is -5.68%.

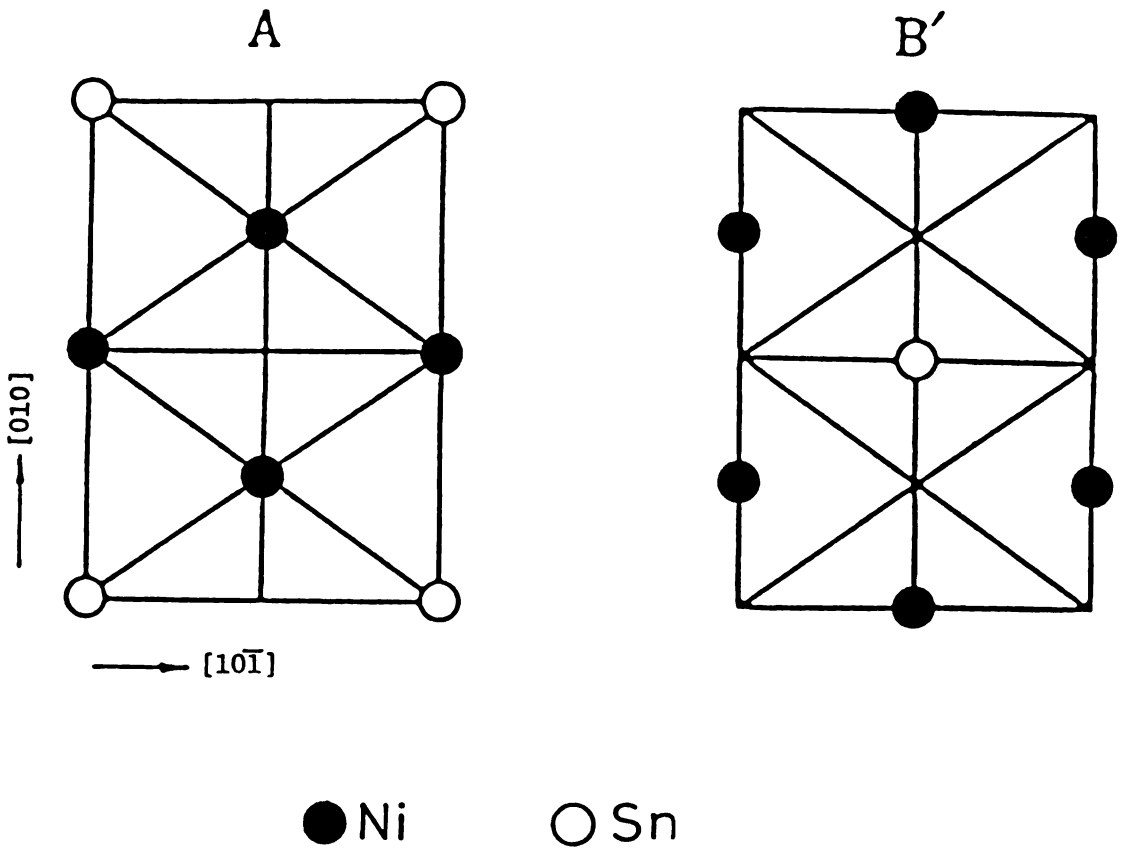

Figure 3.1 The atom positions on (101) plane in the DO_3-type structure.

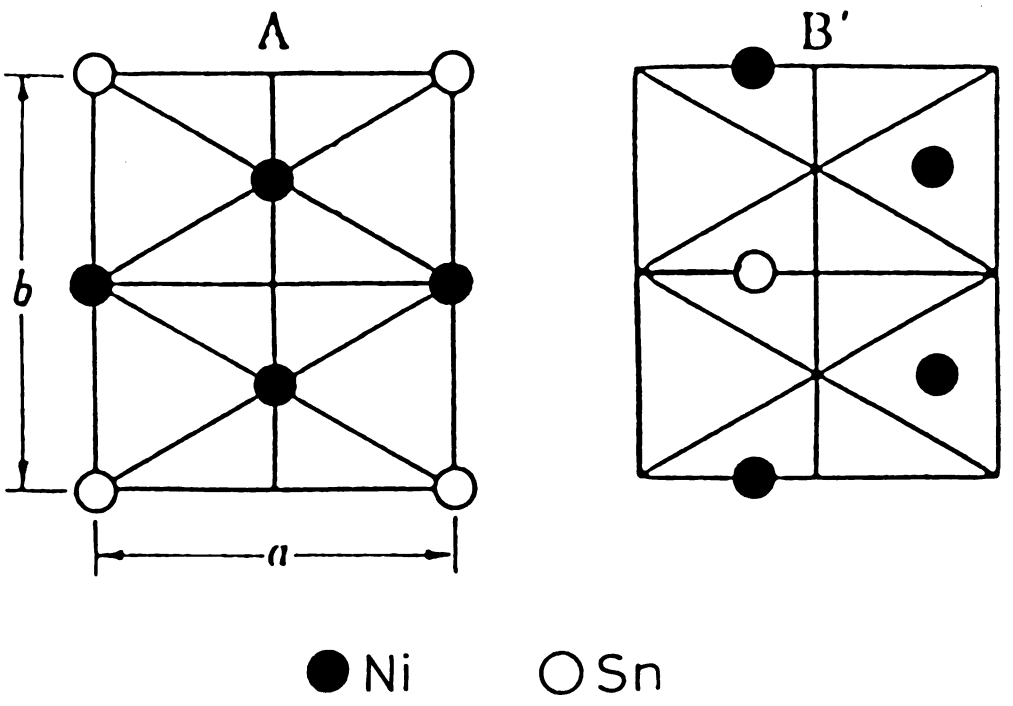

Figure 3.2 The atomic positions on (001) plane in 2H-type structure.

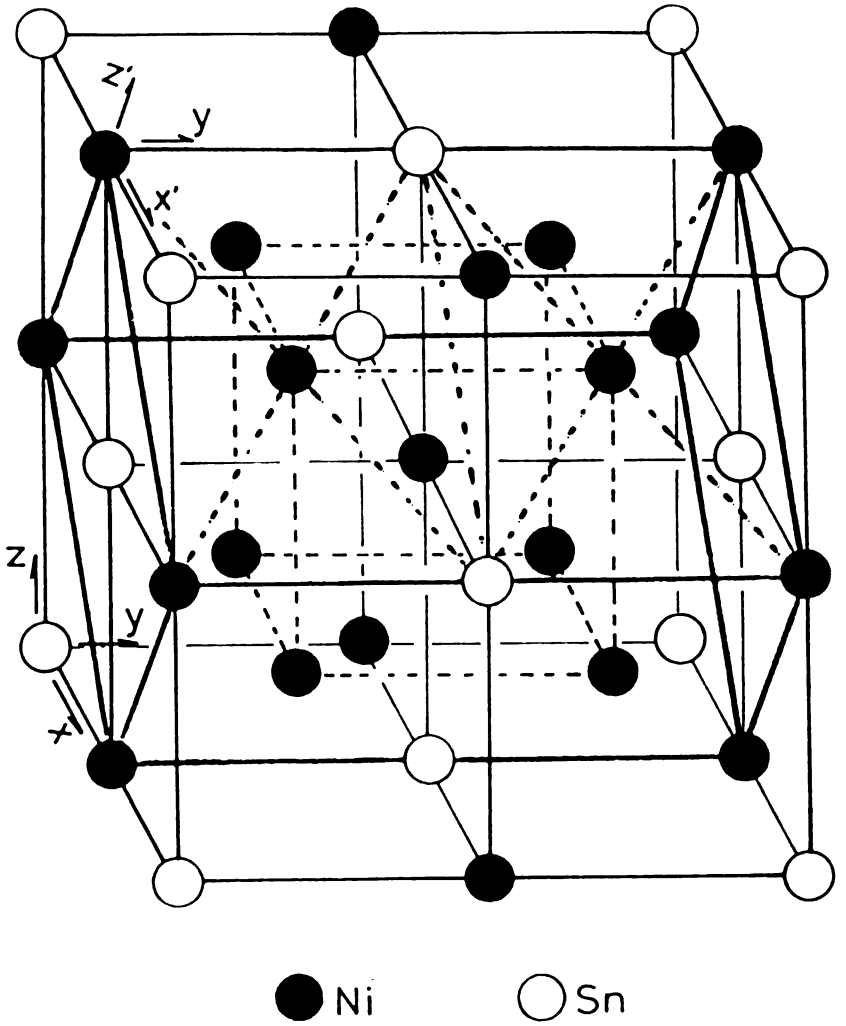

Figure 3.3 The 2H-type structure ("—" line) generated from the tetragonal lattice in the unit cell of the DO_3-type structure.

As shown in previous section, the 2H-type martensites contain $(121)_{2H}$ twins. Thus, this twinning is considered to be the lattice invariant shear. From the lattice correspondence of the parent and martensite, the $(121)_{2H}$ twinning plane is found to be parallel to the $(110)_{DO_3}$ plane. In Figure 3.4 a pair of martensite variants having a twin-relationship with respect to the $(110)_{DO_3}$ plane were drawn.

3.1.2 Phenomenological Analysis Based on the Strain Energy Minimization Criterion

According to Mura et al [14] and Kato et al's [10] analysis based on the strain energy minimization criterion, if the transformation strain ε^T_{ij}(Bain strain plus lattice invariants strain) in an x_1-x_2-x_3 cartesian coordinate system satisfies the condition of

$$\varepsilon^T_{11} = \varepsilon^T_{22} = \varepsilon^T_{12} = 0 , \qquad (3.2)$$

the strain energy becomes minimum(zero) and the condition in equation (3.2), with the x_3-axis as an invariant plane(habit plane) normal, is equivalent to the invariant plane condition in the phenomenological theory. As shown in equation(3.1), the Bain strain in the martensite becomes

$$\varepsilon^1_{ij} = \begin{bmatrix} \varepsilon_1 & 0 & 0 \\ 0 & \varepsilon_2 & 0 \\ 0 & 0 & \varepsilon_3 \end{bmatrix} \qquad (3.3)$$

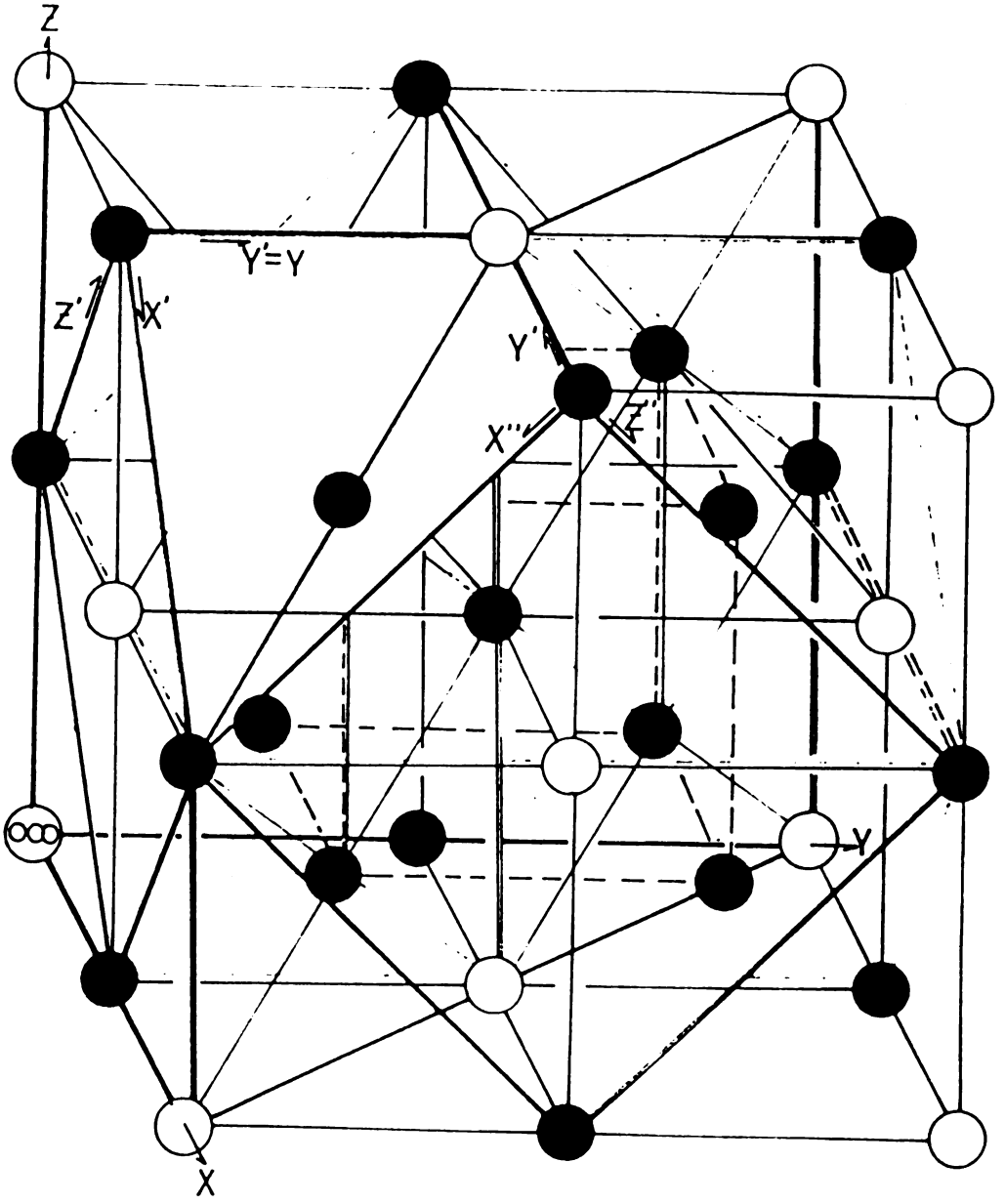

Figure 3.4 A pair of martensite variants having a twin-relationship with respect to the $(110)_{DO_3}$ plane.

where the coordinate system is taken along the principle axes of the DO_3 lattice. As can be seen in equation(3.1), $\varepsilon_1, \varepsilon_2 > 0$ (expansion) $\varepsilon_2 < 0$ (contraction). Equation(3.3) can be changed by similarity transformation based on the x'-y-z' system in the parent phase as

$$\varepsilon_{ij}^{1} = \begin{bmatrix} (\varepsilon_1 + \varepsilon_3) / 2 & 0 & (-\varepsilon_1 + \varepsilon_3) / 2 \\ 0 & \varepsilon_3 & 0 \\ (-\varepsilon_1 + \varepsilon_3) / 2 & o & (\varepsilon_1 + \varepsilon_3) / 2 \end{bmatrix}_{\beta} \quad (3.4)$$

where ε_{ij}^{1} is the Bain strain of variant 1. As shown in Figure 2.11 and 3.6, the lattice variant shear for the martensite domonantly occurs by $(121)_{2H}$ twinning. Thus, the twinned variant should have the Bain strain as

$$\varepsilon_{ij}^{2} = \begin{bmatrix} \varepsilon_2 & 0 & 0 \\ 0 & (\varepsilon_1 + \varepsilon_3) / 2 & (\varepsilon_1 - \varepsilon_3) / 2 \\ 0 & (\varepsilon_1 - \varepsilon_3) / 2 & (\varepsilon_1 + \varepsilon_3) / 2 \end{bmatrix}_{\beta} \quad (3.5)$$

by using the x" -$\bar{x}$ -z" system in the parent phase where ε_{ij}^{2} is the Bain strain of variant. If the volume fraction of the variant is defined as $f(0 < f < 1)$, which is to be determined, then the total transformation strain in the β_1-system, ε_{ij}^{T}, can be written as

$$\varepsilon_{ij}^{T} = f\varepsilon_{ij}^{1} + (1-f)\varepsilon_{ij}^{2} \quad (3.6)$$

From equation (3.3) and (3.4), ε_{ij}^{T} can be obtained :

$$\varepsilon_{ij}^{T} = \begin{bmatrix} \frac{f(\varepsilon_1 + \varepsilon_3)}{2} + (1-f)\varepsilon_2 & 0 & \frac{-\varepsilon_1 + \varepsilon_3}{2} \\ 0 & f\varepsilon_2 + \frac{(1-f)(\varepsilon_1 + \varepsilon_3)}{2} & \frac{(1-f)(\varepsilon_1-\varepsilon_3)}{2} \\ \frac{f(-\varepsilon_1 + \varepsilon_3)}{2} & \frac{(1-f)(\varepsilon_1-\varepsilon_3)}{2} & \frac{(\varepsilon_1+\varepsilon_3)}{2} \end{bmatrix}$$

$$= \begin{bmatrix} \varepsilon_{11}^{T} & 0 & \varepsilon_{13}^{T} \\ 0 & \varepsilon_{22}^{T} & \varepsilon_{23}^{T} \\ \varepsilon_{31}^{T} & \varepsilon_{32}^{T} & \varepsilon_{33}^{T} \end{bmatrix} \qquad (3.7)$$

By rotating the coordinate system, we can find a new x_1-x_2-x_3 system in which the total transformation strain(3.7) satisfies the habit plane condition of equation(3.2). Since $\bar{H}$ becomes parallel to the x_3-axis in this new system, i.e.

$$\bar{H} = [\sin\theta\cos\phi \ , \ \sin\theta\sin\phi \ , \ \cos\theta]\beta \qquad (3.8)$$

We have three unknown parameters θ , ϕ , f which can be solved easily and the results become :

$$\tan^2\phi = -\varepsilon_{22}^{T} / \varepsilon_{11}^{T} \qquad (3.9)$$

$$\tan\theta = \sin\phi(\varepsilon_{11}^{T} - \varepsilon_{22}^{T}) / \varepsilon_{13}^{T}\tan\phi - \varepsilon_{23}^{T} \qquad (3.10)$$

$$f = 1/2 \pm \sqrt{A^2+16A\varepsilon_1\varepsilon_2\varepsilon_3} / 2A \qquad (3.11)$$

where $A = 3\varepsilon_2(\varepsilon_1-\varepsilon_3)^2 - 2(\varepsilon_1-\varepsilon_2)(\varepsilon_2-\varepsilon_3)(\varepsilon_3+\varepsilon_1)$. From equation(3.9), (3.10) and (3.11) the habit plane normal and the volume fraction of the variant 1 were calculated by using the eigen strain as following

$\phi = 70.329$

$\theta = -56.17$

$f = 0.8565$

$$\bar{H} = \begin{bmatrix} -0.2796 \\ -0.7822 \\ 0.5567 \end{bmatrix}$$

$\phi = -70.329$

$\theta = -59.27$

$f = 0.8159$

$$\bar{H} = \begin{bmatrix} -0.2894 \\ 0.8094 \\ 0.5110 \end{bmatrix}$$

3.2 Experimental Determination of Habit Plane by Means of New Method

3.2.1 Proposal of New Method

As mentioned in the introductory part, it is impossible to retain the high temperature parent phase of Ni_3Sn to room temperature. Thus, it would be difficult to get the crystallographic data between parent and martensite phases, unless some special techniques were employed. Here, a new method is proposed to determine not only crystal orientation of parent phase before transformation but also the habit plane of martensites, only by measuring several angles between paired variants.

Figure 3.5 shows the fundamental ideas of the method. $\bar{p}$[HKL] is the normal to the specimen surface,i.e.,the normal to the parent phase. Here, habit plane normals are expressed by $\bar{i}$ and $\bar{j}$, which are assumed to have the same type of indeces. This assumption can be acceptable generally. All vectors $\bar{p}$,$\bar{i}$ and $\bar{j}$ are to be determined as follows.

If $\bar{p}$, $\bar{i}$ and $\bar{j}$ are all unit vectors, $\bar{q}$ and $\bar{r}$ can be obtain from vector products of $\bar{p}$ and $\bar{i}$, $\bar{p}$ and $\bar{j}$ such as

$$\bar{q} = \bar{p} \times \bar{i} \,/\, |\bar{p} \times \bar{i}|$$
$$\bar{r} = \bar{p} \times \bar{j} \,/\, |\bar{p} \times \bar{j}| \quad .$$

Vectors $\bar{q}$ and $\bar{r}$ express trace of martensite variants. The angle ϕ_{ij} between the two traces of variants(i,j) can be obtained from a dot product of the two vectors $\bar{q}$ and $\bar{r}$ as

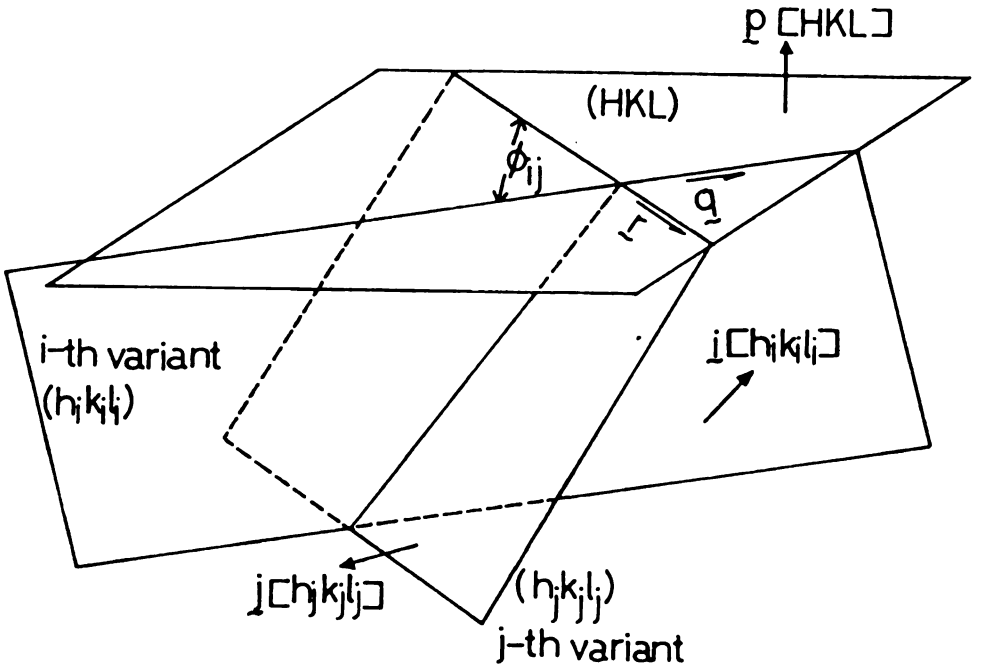

Figure 3.5 Model for the fundamental ideas to obtain the crystallographic data between parent and martensite phases.

$$\text{acos}(\bar{q} \cdot \bar{r}) = \phi_{ij}$$

The angle ϕ_{ij} is experimentally measurable from optical micrographs of martensites. Since any vector can be expressed by two independent variables and since it was already assumed that $\bar{i}$ and $\bar{j}$ have equivalent indices, total independent variables are four. Thus, at least five martensite variants are necessary to determine four independent variables.

In other words, knowing independent angles between paired variants, we can determine not only the surface normal of the parent phase $\bar{p}$ before the martensitic transformation but also the habit plane normal $\bar{i}$ or $\bar{j}$. To find out the desired combination of $\bar{i}$ and $\bar{j}$, computer calculation was employed. The following experiments were carried out to obtain independent angles necessary for the computer calculation.

3.2.2 Experimental Procedures

A rectangular parallel piped specimen was prepared from the Ni_3Sn ingot in order that two surface trace analysis can be done. By the similar processes mentioned in the previous section, acicular martensites were formed. To make surface observation easily, large grains were made by annealing for 40hrs at 1050°C. Surface observation was carried out on two surfaces(A and B) in one grain, perpendicular to each other. Angles between paired traces of martensite variants on both surface A and B were measured.

3.2.3 Experimental Results

Figure 3.6(a) and (b) show the optical micrographs of Ni_3Sn martensites surface A and B. Angles between two traces of these martensite variants measured, ϕ_{ij}, are shown in Table 3.1. Using values of ϕ_{ij} measured, the vectors $\bar{p}$ and $\bar{t}$ could be determined. In the present research, vector $\bar{t}$ will be assumed first as the first step in determing vector $\bar{p}$. Three different vectors were chosen as vector $\bar{t}$ from the following reasons.

Recently, the habit plane of the martensite in Cu-Al-Ni alloy was determined by means of transmission microscopy [15]. The habit plane reported was between {122} and {133}. Since Ni_3Sn alloy and Cu-Al-Ni alloy has the same crystal structure for both parent and martensite phases, the habit plane $\bar{t}$ was assumed to be {122} and {133}. {112} was also chosen as a habit plane for extra example of the computer calculation in determing vector $\bar{p}$. The determination of the vector was carried out in a following way.

As mentioned above, firstly the habit plane $\bar{t}$ was assumed and then actually $\bar{t}$ was chosen as one of the family of the habit plane. Then $\bar{p}$ was chosen to calculate all angles ϕ_{ij} for the other eleven variants of the family. Then, values of angles ϕ_{ij} measured experimentally were compared with those of angles ϕ_{ij} calculated. If all of measured angles ϕ_{ij} are well explained within an allowance of a given angle with reapect to the calculated angles ϕ_{ij}, the computer tells us that this vector $\bar{p}$ might be reasenable as the plane normal of the parent phase. Choice of $\bar{p}$ was carried out systematically in the whole area of the standard triangle of

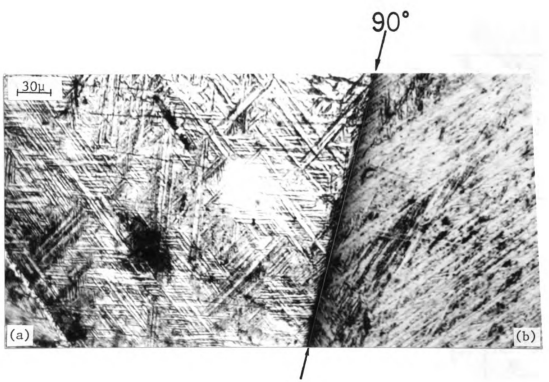

Figure 3.6 (a)(b) The optical micrographs of Ni_2Sn alloy martensite phase on surface A and B, which are perpendicular to each other.

Table 3.1 The observed angles between two traces of Ni_3Sn martensite variants.

from surface A

	(1)	(2)	(3)	(4)	(5)
(1)	-	46.5	86	85.5	53
(2)	46.5	-	40	47.5	80
(3)	86	40	-	8.5	40
(4)	85.5	47.5	8.5	-	32.5
(5)	53	80	40	32.5	-

from surface B

	(1)	(2)	(3)	(4)	(5)	(6)
(1)	-	47	63.3	87	66.5	70
(2)	47	-	16.5	45	66	23
(3)	63.3	16.5	-	28.5	49.5	7.0
(4)	87	45	28.5	-	20.5	22.7
(5)	66.5	66	49.5	20.5	-	43
(6)	70.0	23.0	7.0	22.5	43	-

stereoprojection, [001]-[011]-[$\bar{1}$11], shown in Figure 3.7. If no vector $\bar{p}$ is informed, the first assumption of vector $\bar{i}$ is considered to be wrong under a given allowance condition. Apendix C shows an example of the computer programs employed. In this program, vector $\bar{i}$ was assumed to be (122) and an angle allowance was within $\pm 1.5^{o}$. In this case, reasonable surface normals $\bar{p}$ were obtained, which will be shown later. On the other hand, when {133} and {112} were assumed to be as the habit plane normals, and when the same angle allowance of $\pm 0.5^{o}$ was permitted, no surface normal $\bar{p}$ was obtained. Thus, in present research it can be conclude that (122) plane is a most probable habit plane.

Table 3.2 shows some examples of angles ϕ_{ij} obtained for two surfaces by assuming {122} habit plane. As it can be seen from this table, all of the observed angles are in good agreement with the calculated angles.

For these two surfaces, all surface normals $\bar{p}$ selected by computer were plotted in Figure 3.8. These two surfaces A and B were from one grain and were perpendicular to each other. Although these two surface normals $\bar{p}$ were independently determined, the angle between these two calculated normals is about 90^{o}, which is in good agreement with the directly measured angle. In Figure 3.9 , the surface normals([$\bar{3}$ 13 17] for A and [$\bar{9}\bar{5}$2] for B) and habit planes determined were shown.

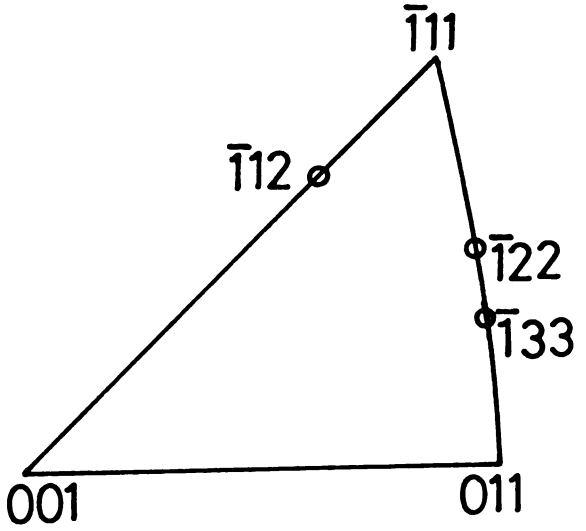

Figure 3.7 The area of the standard triangle of stereoprojection.

Table 3.2 Examples of angles ϕ obtained for two surfaces by assuming (122) habit plane

surface A

ϕ_{cal} : angle between (122) and other {122}

{122}	$(1\bar{2}2)$	$(2\bar{2}1)$	$(2\bar{1}2)$	$(12\bar{2})$	(122)	$(\bar{2}21)$
$\phi_{cal}(^\circ)$	84.77	63.97	58.67	56.33	47.04	45.13
{122}	$(21\bar{2})$	$(22\bar{1})$	(212)	(221)	$(\bar{2}12)$	
$\phi_{cal}(^\circ)$	32.29	31.96	25.59	8.31	1.07	

ϕ_{ij} : measured angles

85.5, 47.5, 32.5, 8.5

surface B

ϕ_{cal} : angle between (221) and other {221}

{221}	$(22\bar{1})$	$(2\bar{2}1)$	$(1\bar{2}2)$	$(\bar{2}12)$	$(12\bar{2})$	$(\bar{2}21)$
$\phi_{cal}(^\circ)$	86.59	85.18	76.34	67.32	65.46	45.58
{221}	(212)	$(21\bar{2})$	$(\bar{1}22)$	$(\bar{2}12)$	(122)	
$\phi_{cal}(^\circ)$	29.71	23.77	21.04	19.59	1.23	

ϕ_{ij} : measured angles

87, 45, 28.5, 22.7, 20.5

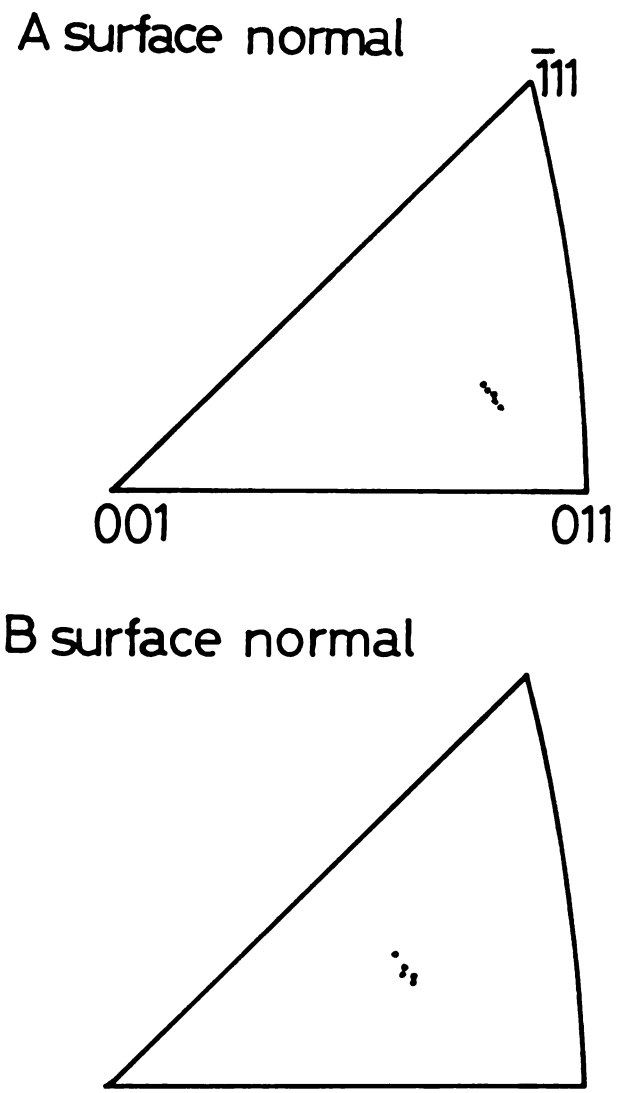

Figure 3.8 All surface normals $\bar{p}$ selected by computer.

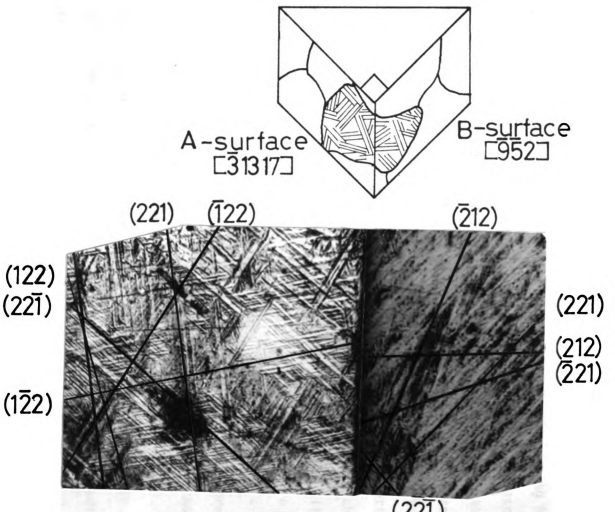

Figure 3.9 The surface normals and habit planes on two surfaces A and B on one grain.

4 DISCUSSION

It was observed that the high temperature DO_3-structure martensitically when quenched rapidly and to the $Mg_3Cd(DO_{19})$-type structure massively when cooled slowly. Thus, it is obvious that no high temperature phase can be retained in this binary alloy regardless cooling rate. Recently, Kachi and Murakami [16] investigated the phase stability of Ni_3Sn high temperature phase by substituting Ni with Cu. They reported that both the parent and martensite phases coexisted at room temperature in a range where Cu composition was between 18 and 21 at%. Since the best way experimentally to determine the orientation of the habit plane of martensites is obviously to retain the parent phase with the martensite phase, trials of getting the retained parent phase were extensively done according to Kachi and Murakami's reports. However, no coexistance of the martensite and parent phases was obtained. Although the DO_3-parent phases were able to be retained in a range of Cu of 18 to 24 at%, those DO_3-phases were found not to transform even if temperature was lowered up to the liquid nitrogen temperature. Instead, it was found that when the DO_3-phases were cooled slowly(actually furnace-cooled), Widmannstatten structures were found to be very stable up to around 400°C. The crystal structure of the Widmannstatten was not determined yet.

The new method was proposed to determine the habit plane of martensites by measuring only angles between paired martensite

variants, without knowing the surface orientation of the parent phase. This method may be called "computer-aided trace analysis method", because without computer it would be almost impossible to determine the habit plane of the martensite. This method is applicable under the following two conditions : (1) all martensite variants in one alloy system have the same type of indeces, and (2) at least five different variants should be observed on a surface within a grain.

Using this method, we can also obtain the surface orientation $\bar{p}$ of the parent phase at a same time. By comparing the actual angle between two surfaces(A and B) with the corresponding angle calculated from the two surface orientations $\bar{p}$ obtained, the validity of the method proposed was examined. As shown in Figure 3.10, the angle calculated from the obtained vectors $\bar{p}$ was about 90° and the angle measured directly from the specimen was also 90°. The results were in very good agreement. In order to make sure of the validity of this method more, however it is necessary to examine whether this method is applicable to other systems, whose habit planes have been known already. This will be carried out in the near future.

The phenomenological theory based on the strain energy minimization criterion [13] was employed to predict the habit plane of Ni_3Sn martensite. Using this theory, two habit planes and volume fraction of twinning variants were able to be obtained. In Figure 3.10 one of the two habit plane normals obtained was plotted.

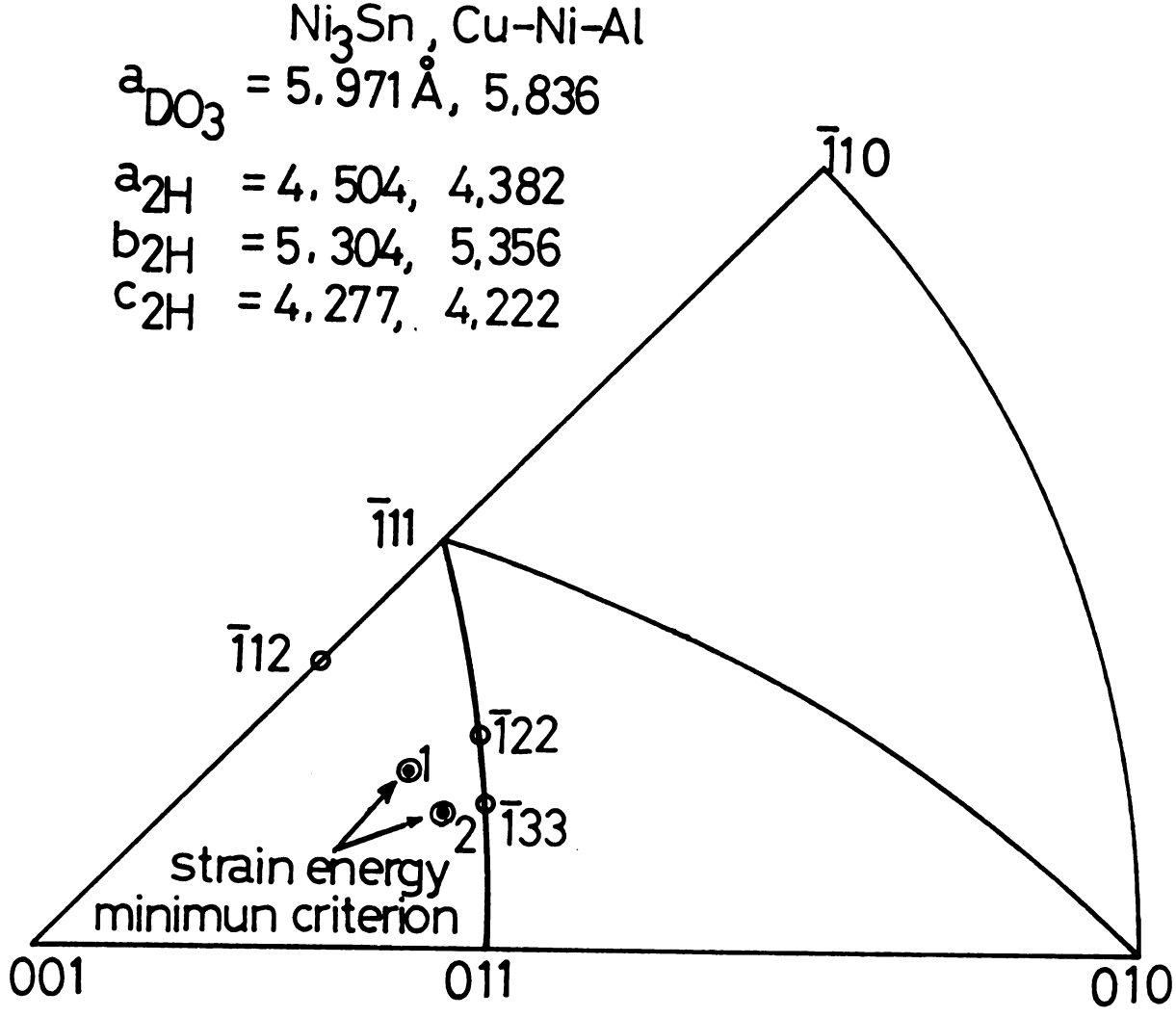

Figure 3.10 Habit planes, (122) and strain energy minimization criterion, and the lattice parameters. "1" is for Ni_3Sn alloy. "2" is for Cu-Ni-Al alloy.

This was because the plotted habit plane was corresponding to the large volume fraction of twinning variants. The volume fraction calculated was 82%, which was in pretty good agreement with that (about 75%) measured from Figure 3.4 and 2.11. In Figure 3.10 another habit plane normal calculated for Cu-Ni-Al alloy [15] was also plotted. As can be seen, this habit plane normal is very close to {122} compared with that of the present alloy. This diffrence between the two alloys may result from the accuracy of lattice parameters for the DO_3-parent phases ; the lattice parameter of Cu-Ni-Al was measured at room temperature [15], while that of Ni_3Sn was measured at 960°C [4] and extrapolated to room temperature by considering thermal expansion. From the habit plane observations on Ni_3Sn and Cu-Ni-Al alloys it can be concluded that the habit plane of 2H-type martensites transformed from DO_3 structure is {122} or close to {122}.

5 SUMMARY

Martensites of Ni_3Sn alloy produced by quenching from 1050°C were investigated crystallographically. The results obtained can be summarized as follows :

1. The crystal structure of the martensite Ni_3Sn alloy was determined as an ordered orthorhombic structure, β-Cu_3Ti-type(2H), by means of electron diffraction. This structure is identical to that determined by means of X-ray diffraction.
2. A new method was proposed to determine the habit plane of the martensite for cases where none or a small amount of parent phase can be retained. This method can be applicable if at least five variants are observed on a surface of one grain.
3. The habit plane of the Ni_3Sn martensite was determined as {122} plane using the new method proposed. Phenomenological theory based on the strain energy minimization criterion was also employed to determine the habit plane. The angle difference between these two habit plane normals determined is considered to be pretty small.

REFERENCES

1. Hansen, M. and Anderko, K., Constitution of Binary Alloys, McGraw-Hill, New York, Toronto, London, (1958), 1042.

2. Shunk,F.A., Constitution of Binary Alloys, McGraw-Hill, New York, Toronto, London, (1969), 555.

3. Heumann, T., Zeitschrift Metallkunde, 35 (1943), 248.

4. Schubert, K., Burkhardt, W., Esslinger, P., Gunzel,E., Meissner, H.G., Schutt, W., Wegst, J. and Wilkens, M., " Eigige Strukturelle Ergebnisse an Metallischen Phasen ", Naturwissenschaften, 43 (1956), 248.

5. Pak, H., Saburi, T. and Nenno, S., " Martensitic and Massive Transformation in Ni_3Sn Alloy ", J. of Japan Institute Metals, 37 (1973), 1128.

6. Shibata, M. and Ono, K., Acta Metallurgica, 23 (1975), 587.

7. Clarke, D.R., Metallurgical Transactions, 7A (1976), 723.

8. Easterling, K.E. and Tholen, A.R., " Acta Metallurgica ", 24 (1976), 333.

9. Shibata, M. and Ono, K. Acta Metallurgica, 25 (1977), 35.

10. Kato, M., Miyazaki, T. and Sunaga, Y., " Re-Examination of the Elastic Energy and the Phenomenological Crystallography Theory in a Martensitic Transformation ", Scripta Metallurgica, 11 (1977), 915.

11. Wechsler, M.S., Lieberman, D.S. and Read, T.A., " On the Theory of the Formation of Martensite ", Transactions AIME , 197 (1953), 1503.

12. Bowles, J.S. and Mackenzie, J.K., " The Crystallography of Martensite Transactions ", Acta Metallurgica, 2 (1954), 129, 224, 138.

13. Mukherjee, K. and Kato, M., " Lattice Correspondence and Crystallography of Martensites ", ICOMAT-82, Leuven, Belgium, (1982).

14. Mura, T., Mori, T. and Kato, M. " The Elastic Field Caused by a General Ellipsodal Inclusion and the Application to Martensite Formation ", J. Mech. Physics of Solids, 24 (1976), 305.

REFERENCE

15. Otsuka, K. and Shimizu, K., " Morphology and Crystallofraphy of Thermoelastic γ' Cu-Al-Ni Martensite ", Japanese J. Applied Physics.

16. Kachi, S. and Murakami, Y., " Martensitic Transformation and Phase Relation in $Ni_{3-x}Cu_xSn$ and $Ni_{3-x}Mn_xSn$ Alloys ", Sci. Report RITU A29, Suppl. 1 (1981), 73.

APPENDIX A

Interplanar Spacings of Ni_3Sn Martensite

Crystal Structure : Orthorhombic
Unit Cell : a=4.504 A, b=5.304 A, c=4.277 A

hkl	spacing(A^{-1})	hkl	spacing(A^{-1})
0 7 1	1.3403	1 2 4	1.0325
1 7 0	1.3383	0 4 3	1.0299
3 6 1	1.3334	4 1 2	1.0212
6 0 3	1.3321	0 2 4	1.0084
6 0 3	1.3310	3 4 3	1.0062
5 3 2	1.3308	2 3 3	1.0045
0 5 4	1.3279	4 0 2	1.0037
5 1 3	1.3266	1 5 1	.9963
0 7 0	1.3198	4 2 1	.9928
1 3 5	1.3175	2 4 2	.9923
4 5 1	1.3161	3 3 2	.9911
5 0 3	1.3132	3 1 3	.9855
3 6 0	1.3128	1 1 4	.9795
2 2 5	1.3062	0 5 1	.9712
4 1 4	1.3034	1 5 0	.9685
2 6 2	1.3021	3 0 3	.9673
0 3 5	1.2987	4 2 0	.9648
4 5 0	1.2951	1 0 4	.9612
4 0 4	1.2897	0 1 4	.9540
2 4 4	1.2809	0 5 0	.9427
3 3 4	1.2799	4 1 1	.9375
5 3 1	1.2577	0 0 4	.9352
4 3 3	1.2652	1 3 3	.9260
2 1 5	1.2647	4 0 1	.9184
5 2 2	1.2622	1 4 2	.9147
2 5 3	1.2561	2 2 3	.9118
4 4 2	1.2554	4 1 0	.9079
2 0 5	1.2505	2 4 1	.9059
1 2 5	1.2483	3 3 1	.9046
5 3 0	1.2459	0 3 3	.9011
3 5 2	1.2454	3 2 2	.8969
1 6 2	1.2440	4 0 2	.8881
2 6 1	1.2375	2 4 0	.8874
0 2 5	1.2284	3 3 0	.8752
3 4 3	1.2265	2 3 2	.8738
0 5 2	1.2241	2 1 3	.8576
4 4 0	1.2218	3 1 2	.8513
1 1 5	1.2193	2 0 3	.8354
5 1 2	1.2153	1 2 3	.8302
2 6 0	1.2085	1 4 1	.8267
3 2 4	1.2048	3 0 2	.8202
1 5 2	1.2046	3 2 1	.8138
5 0 4	1.2014	0 2 3	.8003
0 4 5	1.1958	0 4 1	.7964
1 5 3	1.1955	1 4 0	.7896
5 2 1	1.1929	1 3 2	.7862
4 2 3	1.1899	3 2 0	.7667
1 4 4	1.1883	1 1 3	.7654
3 0 5	1.1841	2 3 1	.7595
0 1 5	1.1797	2 4 0	.7561
2 3 4	1.1777	2 2 2	.7541
3 5 1	1.1763	1 0 3	.7470
1 6 1	1.1750	3 3 2	.7357
5 2 3	1.1724	3 1 1	.7339
0 5 3	1.1690	0 1 3	.7307
4 4 1	1.1651	2 3 0	.7263
3 1 4	1.1636	3 0 1	.7191
0 6 1	1.1551	0 0 3	.7059
3 5 0	1.1543	3 1 0	.7014
1 6 0	1.1528	2 1 2	.6922
4 3 2	1.1521	3 0 2	.6719
5 1 1	1.1500	1 3 1	.6661
3 4 3	1.1482	1 2 2	.6511
2 5 2	1.1473	1 2 2	.6449
5 0 3	1.1421	2 2 1	.6404
4 3 1	1.1345	0 3 1	.6277
0 6 0	1.1317	1 3 0	.6120
5 1 2	1.1312	0 2 2	.6076
2 3 3	1.1260	2 2 0	.6007
3 3 3	1.1216	0 3 0	.5826
1 5 2	1.1205	1 1 2	.5656
4 0 4	1.1153	2 1 1	.5509
3 2 3	1.1101	1 0 2	.5361
0 4 4	1.1095	0 1 2	.5176
2 2 4	1.1018	2 0 1	.5042
4 3 1	1.0930	1 2 1	.5018
1 5 1	1.0786	2 1 0	.4961
4 2 2	1.0755	0 0 2	.4824
2 5 1	1.0722	2 0 0	.4676
1 4 3	1.0679	0 2 1	.4440
4 3 0	1.0536	1 2 0	.4437
2 1 4	1.0529	0 1 1	.4376
2 5 0	1.0523	1 1 1	.3771
3 2 3	1.0523	1 0 1	.3735
2 0 4	1.0420	0 1 1	.3224
3 4 1	1.0382	1 1 0	.3004
	1.0353	0 0 1	.2913
	1.0330	1 0 0	.2338
		0 1 0	.2220
			.1885

0 0 8	1.8705
3 2 7	1.8068
5 1 6	1.7989
5 0 5	1.7990
2 3 7	1.7977
6 1 5	1.7824
3 1 7	1.7770
4 0 5	1.7762
6 0 6	1.7724
3 0 7	1.7670
4 3 6	1.7540
7 2 6	1.7463
1 3 7	1.7458
2 2 7	1.7372
0 3 7	1.7316
3 4 6	1.7264
6 3 4	1.7231
7 3 5	1.7187
7 1 6	1.7155
5 2 6	1.7085
2 1 7	1.7063
7 0 7	1.7051
1 5 6	1.7047
4 2 6	1.7026
2 0 7	1.5958
1 2 7	1.6941
0 5 6	1.6902
6 4 4	1.6839
0 4 7	1.6795
4 1 6	1.6710
6 2 5	1.6708
7 3 4	1.6703
7 2 5	1.6662
1 1 7	1.6624
4 0 6	1.6603
5 2 6	1.6557
7 3 6	1.6539
2 4 6	1.6535
3 3 6	1.6527
1 4 7	1.6517
4 4 6	1.6505
6 5 5	1.6486
0 5 7	1.6475
3 5 6	1.6429
1 6 6	1.6418
6 1 6	1.6385
6 0 7	1.6367
5 4 5	1.6358
7 1 5	1.6339
6 5 6	1.6320
6 0 6	1.6277
0 6 7	1.6266
5 5 6	1.6231
7 0 7	1.6230
5 5 7	1.6165
7 2 7	1.6163
5 6 6	1.6122
3 6 7	1.6118
6 3 7	1.6083
1 4 7	1.6081
5 6 7	1.6021
6 4 7	1.6006
4 6 7	1.6001
7 2 8	1.5993
3 2 8	1.5981
4 5 7	1.5975
4 5 8	1.5927
5 6 8	1.5849
7 1 8	1.5829
2 3 8	1.5764
4 3 8	1.5733
7 0 8	1.5717
2 5 8	1.5660
7 1 8	1.5656
3 1 8	1.5644
2 7 8	1.5591
5 1 8	1.5579
7 0 8	1.5542
3 0 8	1.5529
6 2 8	1.5520
3 7 8	1.5505
6 4 8	1.5486
3 4 8	1.5424
2 6 8	1.5335
6 4 8	1.5308
5 5 8	1.5296
1 3 8	1.5288
6 3 8	1.5209
2 2 8	1.5190
1 5 8	1.5161
6 1 8	1.5173
4 2 8	1.5150
5 4 8	1.5143
0 3 8	1.5126
4 6 8	1.5123
1 7 8	1.5110
0 8 8	1.5083
6 0 8	1.5055
0 5 8	1.5018
5 2 8	1.4997
3 7 8	1.4967
0 7 8	1.4946
4 4 8	1.4940
3 6 8	1.4684
3 5 8	1.4856
1 6 8	1.4845
2 1 8	1.4835
4 1 8	1.4802
3 7 8	1.4783
5 5 8	1.4750
4 5 8	1.4729
2 0 8	1.4715
1 2 8	1.4595
2 7 8	1.4689
4 0 8	1.4581
0 6 8	1.4578
6 3 8	1.4660
5 1 8	1.4638
6 2 8	1.4513
2 4 8	1.4603
3 3 8	1.4595
4 6 8	1.4571
5 5 8	1.4564
0 2 8	1.4526
5 0 8	1.4516
6 3 8	1.4473
4 6 8	1.4382
1 1 8	1.4328
5 3 8	1.4298
6 1 8	1.4244
5 4 8	1.4212
1 0 8	1.4203
1 7 8	1.4176
0 1 8	1.4155
2 7 8	1.4120
6 2 8	1.4118
1 4 8	1.4088
4 3 8	1.4083
6 2 8	1.4041
2 6 8	1.4032
0 0 8	1.4029
2 5 8	1.4002
0 7 8	1.4002
3 2 8	1.3973
3 6 8	1.3936
2 7 8	1.3925
0 4 8	1.3912
6 2 8	1.3845
4 5 8	1.3770
3 4 8	1.3737
2 3 8	1.3725
5 2 8	1.3662
6 1 8	1.3656
5 4 8	1.3623
4 4 8	1.3599
3 1 8	1.3586
1 7 8	1.3586
6 0 8	1.3525
3 5 8	1.3507
1 6 8	1.3494
1 5 8	1.3463
3 0 8	1.3455
6 1 8	1.3454
4 2 8	1.3437
5 4 8	1.3421

APPENDIX B

Angles between Crystallographic Planes in Ni_3Sn Martensite

Crystal Structure : Orthorhombic

Unit Cell : a=4.504 A , b=5.304 A , c=4.277 A

001	+ + +	+ + -	+ - +	+ - -
001	0.00	180.00	0.00	180.00
010	90.00	90.00	90.00	90.00
011	38.56	141.12	38.56	141.12
012	21.96	158.04	21.96	158.04
013	15.04	164.96	15.04	164.96
021	58.20	121.80	58.20	121.80
023	28.26	151.74	28.26	151.74
031	67.54	112.46	67.54	112.46
032	50.42	129.58	50.42	129.58
100	90.00	90.00	90.00	90.00
101	43.52	136.48	43.52	136.48
102	25.40	154.60	25.40	154.60
103	17.56	162.44	17.56	162.44
110	90.00	90.00	90.00	90.00
111	51.25	128.75	51.25	128.75
112	31.92	148.08	31.92	148.08
113	22.55	157.45	22.55	157.45
120	90.00	90.00	90.00	90.00
121	61.88	118.12	61.88	118.12
122	43.10	136.90	43.10	136.90
123	31.96	148.04	31.96	148.04
130	90.00	90.00	90.00	90.00
131	68.45	111.55	68.45	111.55
132	52.42	127.58	52.42	127.58
133	40.90	139.10	40.90	139.10
201	62.23	117.77	62.23	117.77
203	32.34	147.66	32.34	147.66
210	90.00	90.00	90.00	90.00
211	64.14	115.86	64.14	115.86
212	45.89	134.11	45.89	134.11
213	34.52	145.48	34.52	145.48
221	68.13	111.87	68.13	111.87
223	39.71	140.29	39.71	140.29
230	90.00	90.00	90.00	90.00
231	71.39	108.61	71.39	108.61
232	56.96	123.04	56.96	123.04
233	45.71	134.29	45.71	134.29
301	70.66	109.34	70.66	109.34
302	54.93	125.07	54.93	125.07
310	90.00	90.00	90.00	90.00
311	71.34	108.66	71.34	108.66
312	55.96	124.04	55.96	124.04
313	44.62	135.38	44.62	135.38
320	90.00	90.00	90.00	90.00
321	73.01	106.99	73.01	106.99
322	58.58	121.42	58.58	121.42
323	47.50	132.50	47.50	132.50
331	75.02	104.98	75.02	104.98
332	61.85	118.15	61.85	118.15

010	+ + +	+ + -	+ - +	+ - -
010	0.00	0.00	180.00	180.00
011	51.12	51.12	128.88	128.88
012	68.04	68.04	111.96	111.96
013	74.96	74.96	105.04	105.04
021	31.80	31.80	148.20	148.20
023	61.74	61.74	118.26	118.26
031	22.46	22.46	157.54	157.54
032	39.58	39.58	140.42	140.42
100	90.00	90.00	90.00	90.00
101	90.00	90.00	90.00	90.00
102	90.00	90.00	90.00	90.00
103	90.00	90.00	90.00	90.00
110	49.66	49.66	130.34	130.34
111	59.68	59.68	120.32	120.32
112	69.99	69.99	110.01	110.01
113	75.63	75.63	104.37	104.37
120	30.49	30.49	149.51	149.51
121	40.53	40.53	139.47	139.47
122	53.93	53.93	126.07	126.07
123	62.86	62.86	117.14	117.14
130	21.43	21.43	158.57	158.57
131	29.69	29.69	150.31	150.31
132	42.46	42.46	137.54	137.54
133	52.45	52.45	127.55	127.55
201	90.00	90.00	90.00	90.00
203	90.00	90.00	90.00	90.00
210	66.99	66.99	113.01	113.01
211	69.41	69.41	110.59	110.59
212	73.70	73.70	106.30	106.30
213	77.20	77.20	102.80	102.80
221	53.08	53.08	126.92	126.92
223	65.57	65.57	114.43	114.43
230	38.13	38.13	141.87	141.87
231	41.58	41.58	138.42	138.42
232	48.75	48.75	131.25	131.25
233	55.73	55.73	124.27	124.27
301	90.00	90.00	90.00	90.00
302	90.00	90.00	90.00	90.00
310	74.20	74.20	105.80	105.80
311	75.05	75.05	104.95	104.95
312	76.96	76.96	103.04	103.04
313	78.97	78.97	101.03	101.03
320	60.49	60.49	119.51	119.51
321	61.89	61.89	118.11	118.11
322	65.14	65.14	114.86	114.86
323	68.70	68.70	111.30	111.30
331	51.30	51.30	128.70	128.70
332	55.20	55.20	124.80	124.80

011	+ + +	+ + -	+ - +	+ - -
011	0.00	100.24	77.76	180.00
012	16.82	119.16	60.84	163.08
013	23.84	126.07	53.93	156.16
021	19.32	82.92	97.08	160.68
023	10.62	112.86	67.14	169.38
031	28.66	73.58	106.42	151.34
032	11.54	90.70	89.30	168.46
100	90.00	90.00	90.00	90.00
101	55.63	124.37	55.63	124.37
102	45.32	134.68	45.32	134.68
103	42.09	137.91	42.09	137.91
110	66.03	66.03	113.97	113.97
111	36.47	99.61	80.19	143.53
112	28.89	116.48	63.52	151.11
113	28.99	124.27	55.73	151.01
120	57.25	57.25	122.75	122.75
121	32.44	83.67	96.33	147.56
122	20.28	101.47	78.53	159.72
123	18.78	111.97	68.03	161.22
130	54.25	54.25	125.75	125.75
131	34.42	74.59	105.41	145.58
132	20.31	90.67	89.33	159.69
133	13.84	101.88	78.12	166.16
201	68.74	111.26	68.74	111.26
203	48.87	131.13	48.87	131.13
210	75.80	75.80	104.20	104.20
211	55.93	96.82	83.18	124.07
212	44.11	111.45	68.55	135.89
213	38.70	120.16	59.84	141.30
221	48.16	85.00	95.00	131.84
223	30.86	109.83	70.17	149.14
230	60.41	60.41	119.59	119.59
231	44.75	76.77	103.23	135.25
232	33.04	90.60	89.40	146.96
233	26.23	100.96	79.04	153.77
301	75.06	104.94	75.06	104.94
302	63.43	116.57	63.43	116.57
310	80.16	80.16	99.84	99.84
311	65.73	95.00	85.00	114.27
312	54.73	107.19	72.90	125.27
313	47.61	115.72	64.28	132.39
320	71.99	71.99	108.01	108.01
321	58.45	86.08	93.92	121.55
322	47.95	98.16	81.84	132.05
323	41.07	107.33	72.67	138.93
331	63.58	78.97	101.03	126.42
332	43.49	90.52	89.48	136.51

012	+ + +	+ + -	+ - +	+ - -
012	0.00	136.08	43.92	180.00
013	6.91	143.00	36.99	173.08
021	36.24	99.84	80.16	143.76
023	6.30	129.78	50.22	173.70
031	45.58	90.50	89.50	134.42
032	28.46	107.62	72.38	151.54
100	90.00	90.00	90.00	90.00
101	47.74	132.26	47.74	132.26
102	33.09	146.91	33.09	146.91
103	27.84	152.16	27.84	152.16
110	75.99	75.99	104.01	104.01
111	39.71	113.07	66.93	140.29
112	23.77	131.24	48.76	156.23
113	18.31	139.79	40.21	161.69
120	71.20	71.20	108.80	108.80
121	43.84	98.79	81.21	136.16
122	26.19	117.20	62.80	153.81
123	16.78	128.05	51.95	163.22
130	69.63	69.63	110.37	110.37
131	48.86	90.47	89.53	131.14
132	32.70	106.85	73.15	147.30
133	21.73	118.24	61.76	158.27
201	64.40	115.60	64.40	115.60
203	38.41	141.59	38.41	141.59
210	81.60	81.60	98.40	98.40
211	57.59	105.84	74.16	122.41
212	41.37	122.72	57.28	138.63
213	32.12	132.95	47.05	147.88
221	55.24	96.94	83.06	124.76
223	29.76	123.95	56.05	150.24
230	72.89	72.89	107.11	107.11
231	55.49	90.40	89.60	124.51
232	41.22	105.01	74.99	138.78
233	30.89	115.92	64.08	149.11
301	72.11	107.89	72.11	107.89
302	57.90	122.20	57.80	122.20
310	84.15	84.15	95.85	95.85
311	66.84	101.55	78.45	113.16
312	52.48	115.77	64.23	127.12
313	42.97	126.06	53.94	137.03
320	79.38	79.38	100.62	100.62
321	63.44	95.44	84.56	116.56
322	50.15	109.05	70.95	129.85
323	40.32	119.39	60.61	139.68
331	61.74	90.34	89.66	118.26
332	49.38	102.96	77.04	130.62

013	+ + +	+ + -	+ - +	+ - -
013	0.00	149.91	30.09	180.00
021	43.15	106.76	73.24	136.85
023	13.22	136.69	43.31	166.78
031	52.50	97.41	82.59	127.50
032	35.37	114.54	65.46	144.63
100	90.00	90.00	90.00	90.00
101	45.55	134.45	45.55	134.45
102	29.26	150.74	29.26	150.74
103	22.97	157.03	22.97	157.03
110	80.33	80.33	99.67	99.67
111	42.65	110.26	61.74	137.35
112	24.70	136.96	43.04	155.30
113	17.00	145.84	34.16	163.00
120	77.07	77.07	102.93	102.93
121	49.28	104.94	75.06	130.72
122	30.91	123.53	56.47	149.09
123	20.32	134.50	45.50	159.68
130	76.02	76.02	103.98	103.98
131	55.09	96.97	83.03	124.91
132	38.78	113.42	66.58	141.30
133	27.36	124.87	55.13	152.64
201	63.26	116.74	63.26	116.74
203	35.32	144.68	35.32	144.68
210	84.18	84.18	95.82	95.82
211	59.17	109.26	70.74	120.83
212	41.84	126.82	53.18	138.16
213	31.44	137.58	42.42	148.56
221	58.96	101.76	78.24	121.04
223	31.76	129.46	50.54	148.24
230	78.22	78.22	101.78	101.78
231	60.48	96.00	84.00	119.52
232	45.76	110.81	69.19	134.24
233	34.87	121.89	58.11	145.13
301	71.35	108.65	71.35	108.65
302	56.30	123.70	56.30	123.70
310	85.95	85.95	94.05	94.05
311	67.91	104.01	75.99	112.09
312	53.19	118.82	61.18	126.81
313	42.52	129.62	50.38	137.48
320	82.65	82.65	97.35	97.35
321	66.14	99.20	80.80	113.86
322	52.22	113.23	66.77	127.78
323	41.69	123.93	56.07	138.31
331	65.67	95.01	84.99	114.33
332	52.66	107.91	72.09	127.14

021	+ + +	+ + -	+ - +	+ - -
021	0.00	63.60	116.40	180.00
023	29.94	93.54	86.46	150.06
031	9.34	54.26	125.74	170.66
032	7.78	71.38	108.62	172.22
100	90.00	90.00	90.00	90.00
101	67.53	112.47	67.53	112.47
102	61.57	118.43	61.57	118.43
103	59.84	120.16	59.84	120.16
110	56.63	56.63	123.37	123.37
111	40.63	84.31	95.69	139.37
112	42.43	99.00	81.00	137.57
113	45.76	106.00	74.00	134.24
120	42.92	42.92	137.08	137.08
121	26.58	66.57	113.43	153.42
122	27.73	83.36	96.64	152.27
123	33.41	93.41	86.59	146.59
130	37.71	37.71	142.29	142.29
131	21.94	56.70	123.30	158.06
132	18.50	72.21	107.79	161.50
133	23.61	83.13	96.87	156.39
201	75.79	104.21	75.79	104.21
203	63.56	116.44	63.56	116.44
210	70.60	70.60	109.40	109.40
211	58.08	86.04	93.96	121.92
212	52.75	97.37	82.63	127.25
213	51.51	104.24	75.76	128.49
221	45.02	71.68	108.32	134.98
223	40.81	93.09	86.91	139.19
230	48.05	48.05	131.95	131.95
231	37.00	61.79	118.21	143.00
232	32.04	74.15	105.85	147.96
233	32.17	83.65	96.35	147.83
301	79.95	100.05	79.95	100.05
302	72.37	107.63	72.37	107.63
310	76.62	76.62	103.38	103.38
311	67.17	87.10	92.90	112.83
312	60.87	95.92	84.08	119.13
313	57.47	102.27	77.73	122.53
320	65.25	65.25	114.75	114.75
321	56.33	75.73	104.27	123.67
322	50.80	85.26	94.74	129.20
323	48.34	92.71	87.29	131.66
331	48.12	66.72	113.28	131.88
332	42.81	76.33	103.67	137.19

023	+ + +	+ + -	+ - +	+ - -
023	0.00	123.48	56.52	180.00
031	39.28	84.20	95.80	140.72
032	22.16	101.32	78.68	157.84
100	90.00	90.00	90.00	90.00
101	50.30	129.70	50.30	129.70
102	37.28	142.72	37.28	142.72
103	32.89	147.11	32.89	147.11
110	72.15	72.15	107.85	107.85
111	37.78	108.20	71.80	142.22
112	24.54	125.84	54.16	155.46
113	21.41	134.10	45.90	159.59
120	65.92	65.92	114.08	114.08
121	39.20	93.17	86.83	140.80
122	22.79	111.37	68.63	157.21
123	15.58	122.10	57.90	164.42
130	63.85	63.85	116.15	116.15
131	43.31	84.55	95.45	136.69
132	27.57	100.83	79.17	152.43
133	17.38	112.16	67.84	162.62
201	65.77	114.23	65.77	114.23
203	41.91	138.09	41.91	138.09
210	79.34	79.34	100.66	100.66
211	56.59	102.57	77.43	123.41
212	41.76	118.70	61.30	138.24
213	33.84	126.38	51.62	146.16
221	52.23	92.50	87.50	127.77
223	29.14	118.80	61.20	150.86
230	68.13	68.13	111.87	111.87
231	51.21	85.31	94.69	128.79
232	37.59	99.67	80.33	142.41
233	28.16	110.39	69.61	151.84
301	73.04	106.96	73.04	106.96
302	59.60	120.40	59.60	120.40
310	82.59	82.59	97.41	97.41
311	66.17	99.19	80.81	113.83
312	53.14	112.72	67.28	126.86
313	44.15	122.43	57.57	135.85
320	76.51	76.51	103.49	103.49
321	61.29	91.96	88.04	118.71
322	48.83	105.08	74.92	131.17
323	39.91	115.03	64.97	140.09
331	58.42	86.06	93.92	121.58
332	46.70	98.36	81.64	133.30

031	+ + +	+ + -	+ - +	+ - -
031	0.00	44.92	135.08	180.00
032	17.12	62.04	117.96	162.88
100	90.00	90.00	90.00	90.00
101	73.92	106.08	73.92	106.08
102	69.81	110.19	69.81	110.19
103	68.64	111.36	68.64	111.36
110	53.26	53.26	126.74	126.74
111	45.12	76.86	103.14	134.88
112	50.17	90.46	89.54	129.83
113	54.39	97.09	82.91	125.61
120	37.22	37.22	142.78	142.78
121	28.06	58.51	121.49	151.94
122	34.61	74.62	105.38	145.39
123	41.79	84.41	95.59	138.21
130	30.66	30.66	149.34	149.34
131	19.94	48.27	131.73	160.06
132	23.83	63.34	116.66	156.17
133	31.57	74.07	105.93	148.43
201	79.75	100.25	79.75	100.25
203	71.17	108.83	71.17	108.83
210	68.83	68.83	111.17	111.17
211	60.55	80.89	99.11	119.45
212	58.32	90.38	89.62	121.68
213	58.71	96.32	83.68	121.29
221	45.78	65.62	114.38	134.22
223	47.46	84.93	95.07	132.54
230	43.37	43.37	136.63	136.63
231	35.96	55.03	124.97	144.04
232	35.15	66.35	113.65	144.85
233	38.08	75.31	104.69	141.92
301	82.73	97.27	82.73	97.27
302	77.32	102.68	77.32	102.68
310	75.42	75.42	104.58	104.58
311	68.86	83.33	96.67	111.14
312	65.01	90.30	89.70	114.99
313	63.34	95.46	84.54	116.66
320	62.92	62.92	117.08	117.08
321	56.84	71.11	108.89	123.16
322	54.01	79.09	100.91	125.99
323	53.58	85.55	94.45	126.42
331	47.42	61.37	118.63	132.58
332	44.95	69.69	110.31	135.05

032	+ + +	+ + -	+ - +	+ - -
032	0.00	79.16	100.84	180.00
100	90.00	90.00	90.00	90.00
101	62.48	117.52	62.48	117.52
102	54.86	125.14	54.86	125.14
103	52.59	127.41	52.59	127.41
110	60.07	60.07	119.93	119.93
111	38.01	90.56	89.44	141.99
112	36.43	106.09	73.91	143.57
113	38.76	113.40	66.60	141.24
120	48.38	48.38	131.62	131.62
121	27.62	73.41	106.59	152.38
122	23.21	90.66	89.34	156.79
123	26.86	100.90	79.10	153.14
130	44.16	44.16	135.84	135.84
131	26.05	63.85	116.15	153.95
132	16.83	79.63	100.37	163.17
133	17.95	90.68	89.32	162.05
201	72.73	107.27	72.73	107.27
203	57.43	122.57	57.43	122.57
210	72.47	72.47	107.53	107.53
211	56.70	90.39	89.61	123.30
212	48.72	103.13	76.87	131.28
213	45.92	110.75	69.25	134.08
221	45.55	76.96	103.04	134.45
223	36.01	99.87	80.13	143.99
230	52.68	52.68	127.32	127.32
231	39.33	67.70	112.30	140.67
232	31.18	80.74	99.26	148.82
233	28.49	90.63	89.37	151.51
301	77.82	102.18	77.82	102.18
302	68.52	111.48	68.52	111.48
310	77.88	77.88	102.12	102.12
311	66.25	90.29	89.71	113.75
312	57.95	100.53	79.47	122.05
313	53.06	107.82	72.18	126.94
320	67.69	67.69	112.31	112.31
321	56.68	79.81	100.19	123.32
322	48.99	90.47	89.53	131.01
323	44.73	95.65	81.34	135.27
331	49.71	71.51	108.49	130.29
332	42.23	82.00	98.00	137.77

100	+ + +	+ + -	+ - +	+ - -
100	0.00	0.00	0.00	0.00
101	46.48	46.48	46.48	46.48
102	64.50	64.50	64.50	64.50
103	72.44	72.44	72.44	72.44
110	40.34	40.34	40.34	40.34
111	53.53	53.53	53.53	53.53
112	66.23	66.23	66.23	66.23
113	73.00	73.00	73.00	73.00
120	59.51	59.51	59.51	59.51
121	63.42	63.42	63.42	63.42
122	69.72	69.72	69.72	69.72
123	74.42	74.42	74.42	74.42
130	68.57	68.57	68.57	68.57
131	70.06	70.06	70.06	70.06
132	73.17	73.17	73.17	73.17
133	76.16	76.16	76.16	76.16
201	27.77	27.77	27.77	27.77
203	57.66	57.66	57.66	57.66
210	23.01	23.01	23.01	23.01
211	34.07	34.07	34.07	34.07
212	48.63	48.63	48.63	48.63
213	58.56	58.56	58.56	58.56
221	44.98	44.98	44.98	44.98
223	60.86	60.86	60.86	60.86
230	51.87	51.87	51.87	51.87
231	54.04	54.04	54.04	54.04
232	58.82	58.82	58.82	58.82
233	63.77	63.77	63.77	63.77
301	19.34	19.34	19.34	19.34
302	35.07	35.07	35.07	35.07
310	15.80	15.80	15.80	15.80
311	24.27	24.27	24.27	24.27
312	37.12	37.12	37.12	37.12
313	47.48	47.48	47.48	47.48
320	29.51	29.51	29.51	29.51
321	33.67	33.67	33.67	33.67
322	42.05	42.05	42.05	42.05
323	50.09	50.09	50.09	50.09
331	42.58	42.58	42.58	42.58
332	47.77	47.77	47.77	47.77

101	+ + +	+ + -	+ - +	+ - -
101	0.00	92.96	0.00	92.96
102	18.12	111.08	18.12	111.08
103	25.95	118.92	25.95	118.92
110	58.34	58.34	58.34	58.34
111	30.32	92.56	30.32	92.56
112	26.75	109.75	26.75	109.75
113	29.43	117.93	29.43	117.93
120	69.55	69.55	69.55	69.55
121	49.47	91.92	49.47	91.92
122	39.81	106.90	39.81	106.90
123	36.85	115.49	36.85	115.49
130	75.43	75.43	75.43	75.43
131	60.31	91.47	60.31	91.47
132	50.08	104.06	50.08	104.06
133	44.53	112.54	44.53	112.54
201	18.71	74.25	18.71	74.25
203	11.18	104.14	11.18	104.14
210	50.67	50.67	50.67	50.67
211	27.55	75.28	27.55	75.28
212	16.30	92.84	16.30	92.84
213	16.93	103.79	16.93	103.79
221	40.78	77.47	40.78	77.47
223	26.72	102.86	26.72	102.86
230	64.84	64.84	64.84	64.84
231	51.05	79.62	51.05	79.62
232	41.25	92.23	41.25	92.23
233	35.83	101.65	35.83	101.65
301	27.14	65.82	27.14	65.82
302	11.41	81.55	11.41	81.55
310	48.50	48.50	48.50	48.50
311	30.71	66.69	30.71	66.69
312	17.26	81.77	17.26	81.77
313	11.03	92.91	11.03	92.91
320	53.18	53.18	53.18	53.18
321	38.28	68.82	38.28	68.82
322	27.20	82.34	27.20	82.34
323	21.30	92.76	21.30	92.76
331	46.01	71.36	46.01	71.36
332	36.49	83.07	36.49	83.07

102	+ + +	+ + -	+ - +	+ - -
102	0.00	129.20	0.00	129.20
103	7.83	137.04	7.83	137.04
110	70.92	70.92	70.92	70.92
111	34.97	108.09	34.97	108.09
112	20.01	126.43	20.01	126.43
113	16.33	135.14	16.33	135.14
120	77.43	77.43	77.43	77.43
121	51.85	103.52	51.85	103.52
122	36.07	120.72	36.07	120.72
123	28.16	130.64	28.16	130.64
130	80.98	80.98	80.98	80.98
131	61.92	100.26	61.92	100.26
132	47.54	115.26	47.54	115.26
133	38.24	125.46	38.24	125.46
201	36.83	92.37	36.83	92.37
203	6.94	122.27	6.94	122.27
210	66.75	66.75	66.75	66.75
211	41.47	92.22	41.47	92.22
212	24.19	110.20	24.19	110.20
213	14.53	121.37	14.53	121.37
221	50.22	91.89	50.22	91.89
223	25.34	119.08	25.34	119.08
230	74.64	74.64	74.64	74.64
231	57.91	91.57	57.91	91.57
232	44.40	105.69	44.40	105.69
233	34.88	116.18	34.88	116.18
301	45.26	83.94	45.26	83.94
302	29.53	99.67	29.53	99.67
310	65.63	65.63	65.63	65.63
311	47.15	84.15	47.15	84.15
312	32.04	99.42	32.04	99.42
313	21.12	110.68	21.12	110.68
320	68.08	68.08	68.08	68.08
321	51.62	84.66	51.62	84.66
322	37.86	98.77	37.86	98.77
323	27.69	109.58	27.69	109.58
331	56.68	85.28	56.68	85.28
332	44.40	97.93	44.40	97.93

103	+ + +	+ + -	+ - +	+ - -
103	0.00	144.87	0.00	144.87
110	76.70	76.70	76.70	76.70
111	39.09	114.67	39.09	114.67
112	21.43	133.44	21.43	133.44
113	14.37	142.40	14.37	142.40
120	81.19	81.19	81.19	81.19
121	54.24	108.32	54.24	108.32
122	36.80	126.25	36.80	126.26
123	27.14	136.71	27.14	136.71
130	83.67	83.67	83.67	83.67
131	63.56	103.86	63.56	103.86
132	48.02	119.61	48.02	119.61
133	37.55	130.42	37.55	130.42
201	44.67	100.20	44.67	100.20
203	14.77	130.10	14.77	130.10
210	73.87	73.87	73.87	73.87
211	48.26	99.55	48.26	99.55
212	30.34	117.65	30.34	117.65
213	19.45	128.91	19.45	128.91
221	55.35	98.14	55.35	98.14
223	28.31	125.91	28.31	125.91
230	79.26	79.26	79.26	79.26
231	61.84	96.75	61.84	96.75
232	47.47	111.32	47.47	111.32
233	36.96	122.16	36.96	122.16
301	53.09	91.78	53.09	91.78
302	37.36	107.51	37.36	107.51
310	73.12	73.12	73.12	73.12
311	54.54	91.72	54.54	91.72
312	39.26	107.04	39.26	107.04
313	28.05	118.33	28.05	118.33
320	74.77	74.77	74.77	74.77
321	58.02	91.57	58.02	91.57
322	43.85	105.84	43.85	105.84
323	33.10	116.78	33.10	116.78
331	62.05	91.39	62.05	91.39
332	49.26	104.38	49.26	104.38

110	+ + +	+ + -	+ - +	+ - -
110	0.00	0.00	80.67	80.67
111	38.75	38.75	82.74	82.74
112	58.08	58.08	85.08	85.08
113	67.45	67.45	86.44	86.44
120	19.17	19.17	99.85	99.85
121	33.58	33.58	98.68	98.68
122	49.81	49.81	96.71	95.71
123	60.00	60.00	95.19	95.19
130	28.23	28.23	108.90	108.90
131	34.69	34.69	107.60	107.60
132	45.72	45.72	104.88	104.88
133	54.77	54.77	102.25	102.25
201	47.59	47.59	47.59	47.59
203	65.94	65.94	65.94	65.94
210	17.33	17.33	63.34	63.34
211	30.79	30.79	66.19	66.19
212	46.73	46.73	71.21	71.21
213	57.25	57.25	75.27	75.27
221	21.87	21.87	81.35	81.35
223	50.29	50.29	84.06	84.06
230	11.53	11.53	92.20	92.20
231	21.28	21.28	92.09	92.09
232	34.77	34.77	91.85	91.85
233	45.46	45.46	91.58	91.58
301	44.01	44.01	44.01	44.01
302	51.40	51.40	51.40	51.40
310	24.53	24.53	56.14	56.14
311	30.47	30.47	58.14	58.14
312	41.08	41.08	62.50	62.50
313	50.28	50.28	66.96	66.96
320	10.82	10.82	69.85	69.85
321	20.05	20.05	70.77	70.77
322	33.05	33.05	72.91	72.91
323	43.60	43.60	75.29	75.29
331	14.98	14.98	80.99	80.99
332	28.15	28.15	81.79	81.79

111	+ + +	+ + -	+ - +	+ - -
111	0.00	77.51	[illegible]	[illegible]
112	19.33	[illegible]	[illegible]	[illegible]
113	[illegible]	[illegible]	[illegible]	[illegible]
120	42.56	[illegible]	[illegible]	[illegible]
121	19.15	[illegible]	[illegible]	[illegible]
122	16.19	[illegible]	[illegible]	[illegible]
123	22.93	[illegible]	[illegible]	[illegible]
130	[illegible]	[illegible]	[illegible]	[illegible]
131	[illegible]	[illegible]	[illegible]	[illegible]
132	[illegible]	[illegible]	[illegible]	[illegible]
133	[illegible]	[illegible]	[illegible]	[illegible]
201	[illegible]	[illegible]	[illegible]	[illegible]
203	[illegible]	[illegible]	[illegible]	[illegible]
210	[illegible]	[illegible]	[illegible]	[illegible]
211	[illegible]	[illegible]	[illegible]	[illegible]
212	[illegible]	[illegible]	[illegible]	[illegible]
213	[illegible]	[illegible]	[illegible]	[illegible]
221	[illegible]	[illegible]	[illegible]	[illegible]
223	[illegible]	[illegible]	[illegible]	[illegible]
230	[illegible]	[illegible]	[illegible]	[illegible]
231	[illegible]	[illegible]	[illegible]	[illegible]
232	[illegible]	[illegible]	[illegible]	[illegible]
233	[illegible]	[illegible]	[illegible]	[illegible]
301	[illegible]	[illegible]	[illegible]	[illegible]
302	[illegible]	[illegible]	[illegible]	[illegible]
310	[illegible]	[illegible]	[illegible]	[illegible]
311	[illegible]	[illegible]	[illegible]	[illegible]
312	[illegible]	[illegible]	[illegible]	[illegible]
313	[illegible]	[illegible]	[illegible]	[illegible]
320	[illegible]	[illegible]	[illegible]	[illegible]
321	[illegible]	[illegible]	[illegible]	[illegible]
322	[illegible]	[illegible]	[illegible]	[illegible]
323	[illegible]	[illegible]	[illegible]	[illegible]
331	[illegible]	[illegible]	[illegible]	[illegible]
332	[illegible]	[illegible]	[illegible]	[illegible]

112	+ + +	+ + -	+ - +	+ - -
112	0.00	116.16	40.02	132.47
113	9.37	125.53	35.24	139.66
120	60.04	60.04	95.19	95.19
121	32.81	87.66	71.32	116.67
122	16.06	106.17	56.08	132.96
123	10.11	117.12	47.76	140.18
130	62.24	62.24	99.56	99.86
131	42.31	82.53	81.67	117.69
132	27.52	98.54	67.55	130.80
133	18.82	109.67	58.04	138.91
201	41.23	92.23	41.23	92.23
203	21.13	120.11	21.13	120.11
210	59.69	59.69	76.28	76.28
211	34.48	85.18	54.29	99.02
212	17.60	103.20	40.44	114.86
213	9.81	114.42	33.51	124.40
221	36.21	79.95	66.69	103.69
223	7.79	108.37	44.85	126.74
230	58.80	58.80	91.16	91.16
231	40.96	76.69	75.93	106.37
232	26.23	91.63	63.53	119.67
233	15.52	102.82	54.68	127.39
301	48.59	84.31	48.59	84.31
302	35.16	99.08	35.16	99.08
310	61.25	61.25	72.87	72.87
311	43.34	79.39	56.59	89.57
312	29.11	94.39	44.01	103.76
313	19.51	105.44	35.85	113.40
320	58.71	58.71	79.51	79.51
321	41.87	75.60	65.03	94.23
322	27.67	89.96	53.28	106.69
323	17.00	100.99	44.95	116.05
331	43.10	73.06	72.41	97.65
332	29.93	86.23	61.57	108.99

113	+ + +	+ + -	+ - +	+ - -
113	0.00	134.99	26.75	146.00
120	68.76	68.76	93.76	93.76
121	41.00	96.65	67.83	119.54
122	22.80	115.27	50.99	135.98
123	12.76	126.29	41.51	144.91
130	70.25	70.25	97.14	97.14
131	49.56	90.93	77.54	116.52
132	33.80	107.19	62.30	131.43
133	23.18	118.44	51.98	141.21
201	46.45	99.88	46.45	99.88
203	20.50	128.61	20.50	128.61
210	68.52	68.52	80.09	80.09
211	42.93	94.21	56.11	104.36
212	25.09	112.33	39.97	121.28
213	14.44	123.61	30.86	131.56
221	45.58	89.32	66.32	106.64
223	17.16	117.74	41.39	132.13
230	67.93	67.93	90.54	90.84
231	49.99	85.88	74.24	107.43
232	35.07	100.86	60.59	121.05
233	23.96	112.08	50.55	130.95
301	54.43	91.72	54.43	91.72
302	39.65	106.94	39.65	106.94
310	69.58	69.58	77.66	77.66
311	51.24	87.99	60.13	95.34
312	36.29	103.17	46.05	109.67
313	25.52	114.35	35.16	120.48
320	67.87	67.87	82.41	82.41
321	50.95	84.81	66.66	98.25
322	36.59	99.21	53.54	111.64
323	25.62	110.26	43.83	121.77
331	52.47	82.43	72.52	100.29
332	39.30	95.60	60.52	112.39

120	+ + +	+ + -	+ - +	+ - -
120	0.00	0.00	119.02	119.02
121	28.12	28.12	115.33	115.33
122	46.90	46.90	109.36	109.36
123	58.04	58.04	104.88	104.88
130	9.06	9.06	128.08	128.08
131	22.63	22.63	125.14	125.14
132	38.50	38.50	115.26	115.26
133	49.71	49.71	113.92	113.92
201	63.32	63.32	63.32	63.32
203	74.25	74.25	74.25	74.25
210	36.50	36.50	82.52	82.52
211	43.67	43.67	83.27	83.27
212	54.75	54.75	84.63	84.63
213	62.90	62.90	85.77	85.77
221	28.77	28.77	99.13	99.13
223	52.88	52.88	96.27	96.27
230	7.64	7.64	111.38	111.38
231	19.52	19.52	110.28	110.28
232	33.81	33.81	107.79	107.79
233	44.81	44.81	105.12	105.12
301	61.40	61.40	61.40	61.40
302	65.46	65.46	65.46	65.46
310	43.71	43.71	75.31	75.31
311	46.77	46.77	76.10	76.10
312	53.20	53.20	77.57	77.67
313	59.48	59.48	79.74	79.74
320	30.00	30.00	89.02	89.02
321	34.08	34.08	89.07	89.07
322	42.35	42.35	89.17	89.17
323	50.32	50.32	89.28	89.28
331	24.16	24.16	99.51	99.51
332	33.61	33.61	98.67	98.67

121	+ + +	+ + -	+ - +	+ - -
121	9.00	56.23	98.93	126.83
122	18.78	75.02	87.03	129.53
123	25.93	86.16	80.02	128.76
130	29.43	29.43	122.95	122.95
131	10.85	49.94	109.78	132.60
132	12.13	66.24	98.26	135.93
133	22.11	77.64	90.00	135.43
201	52.01	79.84	52.01	79.84
203	50.39	99.14	50.39	99.14
210	44.85	44.85	83.40	83.40
211	32.49	64.38	72.01	95.86
212	33.17	79.57	65.76	104.21
213	37.41	89.23	63.04	108.86
221	18.44	53.30	67.86	104.39
223	26.52	80.23	74.56	117.32

123	+ + +	+ + -	+ - +	+ - -
230	29.06	29.06	108.75	108.75
231	12.30	46.72	99.21	116.84
232	8.21	61.58	90.72	121.76
233	17.29	72.74	84.32	124.00
301	54.67	74.56	54.67	74.56
302	50.43	84.52	50.43	84.52
310	50.39	50.39	77.08	77.08
311	40.99	63.05	66.74	86.58
312	37.61	74.66	63.32	94.50
313	38.44	83.54	60.59	103.27
320	40.19	40.19	89.14	89.14
321	29.75	53.64	81.26	97.00
322	26.16	66.04	75.02	103.47
323	28.17	75.83	70.76	107.90
331	22.09	46.93	91.37	105.52
332	16.89	59.19	84.87	110.91

122	+ + +	+ + -	+ - +	+ - -
122	0.00	93.90	72.14	137.43
123	11.14	104.94	63.54	142.65
130	47.57	47.57	114.92	114.92
131	26.88	66.44	97.53	130.96
132	11.46	84.87	83.61	141.19
133	6.44	96.32	73.98	145.87
201	49.69	91.92	49.69	91.92
203	36.64	115.56	36.64	115.56
210	56.59	56.59	84.89	84.89
211	35.54	79.86	66.51	103.79
212	25.50	96.54	55.10	116.36
213	24.10	106.86	49.30	123.45
221	29.44	70.92	80.59	112.36
223	13.08	98.59	60.85	129.52
230	47.38	47.38	104.42	104.42
231	29.57	65.28	90.63	117.56
232	15.03	80.23	79.09	127.36
233	5.95	91.44	70.64	133.48
301	55.32	65.11	55.32	85.11
302	45.31	97.81	45.31	97.81
310	60.40	60.40	80.03	80.03
311	45.44	76.45	66.56	93.99
312	35.11	89.97	56.48	105.38
313	29.93	99.95	50.11	113.45
320	53.72	53.72	89.33	89.33
321	38.81	69.35	77.03	101.67
322	27.67	82.86	67.01	111.76
323	21.63	93.27	59.57	119.00
331	35.69	64.23	85.65	107.55
332	24.00	77.03	76.03	115.59

123	+ + +	+ + -	+ - +	+ - -
123	0.00	116.04	54.27	148.84
130	58.49	58.49	109.05	109.05
131	37.58	79.45	90.00	127.54
132	21.30	95.92	75.00	140.91
133	10.42	107.40	64.69	148.76
201	50.73	99.07	50.73	99.07
203	30.63	124.97	30.63	124.97
210	64.82	64.82	86.05	86.05
211	41.16	89.27	64.40	107.94
212	26.36	106.56	50.21	122.75
213	19.92	117.26	42.43	131.30
221	38.74	81.49	76.58	113.58
223	13.57	109.47	53.50	135.26
230	58.36	58.36	101.12	101.12
231	40.43	76.32	85.48	116.47
232	25.54	91.36	72.49	126.63
233	14.54	102.53	62.98	136.93
301	57.70	91.58	57.70	91.58
302	44.96	105.03	44.98	105.03
310	67.50	67.50	82.20	82.20
311	50.65	84.78	66.51	98.30
312	37.63	99.08	54.12	111.33
313	29.23	109.58	45.72	120.64
320	62.72	62.72	89.48	89.48
321	46.66	79.02	75.14	103.84
322	33.54	92.93	63.26	115.76
323	24.33	103.61	54.56	124.51
331	45.39	74.71	82.92	107.86
332	32.74	87.68	71.31	118.69

130	+ + +	+ + -	+ - +	+ - -
130	0.00	0.00	137.14	137.14
131	21.05	21.05	133.16	133.16
132	37.58	37.58	125.51	125.51
133	49.10	49.10	118.68	118.68
201	71.14	71.14	71.14	71.14
203	78.73	78.73	78.73	78.73
210	45.56	45.56	91.57	91.57
211	50.95	50.95	91.42	91.42
212	59.82	59.82	91.13	91.13
213	66.62	66.62	90.89	90.89
221	35.15	35.15	107.50	107.50
223	55.74	55.74	101.95	101.95
230	16.70	16.70	120.43	120.43
231	24.37	24.37	118.80	118.80
232	36.59	36.59	115.13	115.13
233	46.71	46.71	111.26	111.26
301	69.83	69.83	69.83	69.83
302	72.60	72.60	72.60	72.60
310	52.76	52.76	84.37	84.37
311	55.02	55.02	84.67	84.67
312	59.91	59.91	85.34	85.34
313	64.45	64.45	86.05	86.05
320	39.05	39.05	98.08	98.08
321	42.04	42.04	97.73	97.73
322	48.50	48.50	96.89	96.89
323	55.07	55.07	95.95	95.95
331	31.67	31.67	108.24	108.24
332	34.03	34.03	106.60	106.60

131	+ + +	+ + -	+ - +	+ - -
131	0.00	42.09	129.83	140.12
132	16.53	58.62	120.95	139.57
133	28.05	70.14	120.16	136.02
201	62.03	62.27	62.03	62.27
203	80.93	96.95	80.93	96.95
210	49.20	49.20	91.47	91.47
211	41.67	64.44	82.32	100.35
212	44.02	77.34	76.51	105.57
213	48.23	85.73	73.66	108.08
221	26.25	91.00	98.45	114.46
223	36.71	75.55	85.23	114.06
230	26.63	26.63	116.21	116.21
231	16.02	42.35	109.79	124.12
232	19.05	56.38	101.57	126.31
233	27.04	67.10	95.03	125.10
301	63.55	79.36	63.55	78.36
302	80.96	80.96	80.96	80.96
310	55.62	55.62	84.75	84.75
311	49.45	69.16	78.37	91.52
312	48.91	74.52	77.93	97.19
313	49.29	81.99	77.34	101.03
320	43.55	43.55	97.54	97.54
321	37.96	53.97	91.19	103.32
322	36.32	64.45	85.66	107.41
323	39.02	73.04	81.91	109.54
331	27.48	45.45	101.50	112.64
332	26.56	56.25	95.58	115.85

132	+ + +	+ + -	+ - +	+ - -
132	0.00	75.16	95.27	145.34
133	11.52	86.68	86.31	147.29
201	57.39	91.50	91.50	91.50
203	47.92	111.13	47.92	111.13
210	56.30	56.30	91.65	91.65
211	46.07	76.91	75.73	106.59
212	34.63	91.45	66.47	116.11
213	30.22	100.94	60.60	120.99
221	38.94	80.11	90.64	117.74
223	23.76	91.32	72.23	123.24
230	40.62	40.62	113.67	113.67
231	24.43	57.77	101.14	124.77
232	14.34	72.31	90.23	131.90
233	14.25	85.25	82.04	135.56
301	61.63	85.92	61.63	85.92
302	54.03	88.51	54.03	96.51
310	61.54	61.54	85.54	85.54
311	49.50	74.98	74.41	96.98
312	42.37	86.79	66.08	106.64
313	39.56	96.58	60.75	112.30
320	52.02	52.02	96.40	96.40
321	39.94	65.77	85.89	105.54
322	32.53	76.04	77.12	114.40
323	30.03	87.61	70.74	119.42
331	33.56	56.88	85.19	113.93
332	25.39	70.86	76.49	120.94

133	+ + +	+ + -	+ - +	+ - -
133	0.00	98.20	75.10	152.34
201	55.58	98.07	55.58	98.07
203	39.95	120.71	39.95	120.71
210	62.71	62.71	91.03	91.03
211	46.08	80.20	71.73	110.23
212	31.22	131.56	59.13	122.51
213	25.05	111.23	50.22	129.27
221	35.66	76.38	85.14	118.57
223	19.19	103.29	67.52	135.81
230	51.16	51.16	104.37	104.37
231	33.99	68.71	94.66	123.31
232	20.51	83.47	82.36	135.04
233	12.39	94.52	75.12	139.93
301	61.57	91.41	61.57	91.41
302	50.94	103.80	50.94	103.80
310	66.56	66.56	86.32	86.32
311	51.89	82.33	72.36	100.41
312	41.29	94.44	61.56	111.71
313	35.29	105.05	54.33	119.53
320	59.44	59.44	95.29	95.29
321	45.00	74.61	82.37	107.99
322	34.11	87.72	71.61	118.40
323	27.58	97.58	63.72	125.37
331	41.15	68.78	90.55	113.4
332	30.04	81.24	80.24	120.34

201	+ + +	+ + -	+ - +	+ - -
201	0.00	55.54	[illegible]	55.54
203	29.89	85.43	29.89	85.43
210	35.47	35.47	35.47	35.47
211	20.59	58.01	20.59	58.01
212	24.62	74.90	24.62	74.90
213	32.28	98.55	32.28	98.55
221	36.92	83.10	36.92	83.10
223	37.88	85.84	37.88	85.84
230	56.88	56.88	56.88	56.88
231	48.42	67.94	48.42	67.94
232	44.60	78.22	44.60	78.22
233	44.24	86.23	44.24	86.23
301	6.43	47.11	6.43	47.11
302	7.30	62.84	7.30	62.84
310	31.64	31.64	31.64	31.64
311	17.12	48.89	17.12	48.89
312	14.92	63.60	14.92	63.60
313	21.62	74.55	21.62	74.55
320	39.65	39.65	39.65	39.65
321	29.65	59.11	29.65	59.11
322	21.94	65.53	21.94	65.53
323	20.06	79.59	20.06	79.59
331	36.47	67.91	36.47	67.91
332	36.46	67.91	36.41	67.91

203	+ + +	+ + -	+ - +	+ - -
203	0.00	115.35	0.00	115.35
210	60.50	60.50	60.50	60.50
211	35.75	85.72	35.75	85.72
212	19.66	103.56	19.66	103.56
213	12.80	114.86	12.80	114.86
221	46.12	88.35	46.12	88.35
223	24.43	112.92	24.43	112.92
230	70.71	70.71	70.71	70.71
231	54.87	85.97	54.87	85.97
232	42.48	100.59	42.48	100.59
233	34.27	110.79	34.27	110.79
301	38.32	77.01	38.32	77.01
302	22.59	92.73	22.59	92.73
310	59.02	59.02	59.02	59.02
311	40.71	77.45	40.71	77.45
312	25.92	92.66	25.92	92.66
313	15.66	103.88	15.66	103.88
320	62.26	62.26	62.26	62.26
321	46.21	78.56	46.21	78.56
322	33.10	92.46	33.10	92.46
323	23.93	103.15	23.93	103.15
331	52.25	79.49	52.25	79.49
332	40.70	92.24	40.70	92.24

210	+ + +	+ + -	+ - +	+ - -
210	0.00	0.00	46.01	46.01
211	25.86	25.86	51.32	51.32
212	44.11	44.11	60.09	60.09
213	55.48	55.48	66.82	66.82
221	27.64	27.64	65.39	65.39
223	52.42	52.42	73.34	73.34
230	28.86	28.86	74.87	74.87
231	33.60	33.60	75.63	75.63
232	42.76	42.76	77.36	77.36
233	51.18	51.18	79.23	79.23
301	29.71	29.71	29.71	29.71
302	41.12	41.12	41.12	41.12
310	7.20	7.20	38.81	38.81
311	19.96	19.96	42.42	42.42
312	34.70	34.70	49.76	49.76
313	45.82	45.82	56.81	56.81
320	6.51	6.51	52.52	52.52
321	18.16	18.16	54.41	54.41
322	32.02	32.02	58.72	58.72
323	42.90	42.90	63.35	63.35
331	22.76	22.76	64.34	64.34
332	32.68	32.68	66.70	66.70

211	+ + +	+ + -	+ - +	+ - -
211	0.00	51.72	41.18	66.15
212	18.25	69.97	41.21	81.65
213	29.62	81.34	44.48	90.30
221	16.53	50.50	57.51	77.75
223	27.53	77.68	53.50	94.49
230	37.99	37.99	75.42	76.42
231	27.83	52.07	69.01	84.92
232	26.04	64.96	64.24	92.34
233	29.69	74.95	61.79	97.84
301	22.18	50.42	22.18	50.42
302	21.79	64.70	21.79	64.70
310	26.77	26.77	45.48	45.48
311	9.80	45.07	36.50	58.35
312	10.28	60.29	34.39	70.31
313	20.36	71.54	36.58	79.51
320	26.61	26.61	56.80	56.80
321	10.74	43.31	49.38	66.66
322	7.97	57.62	46.00	75.12
323	17.48	68.62	45.71	83.74
331	19.51	44.19	59.82	73.90
332	15.60	56.52	55.82	81.36

212	+ + +	+ + -	+ - +	+ - -
212	0.00	88.22	32.59	97.26
213	11.37	99.59	31.12	106.91
221	26.45	67.86	56.07	87.72
223	13.26	85.60	42.16	109.24
230	51.03	51.03	79.20	79.20
231	35.59	67.49	56.53	92.12
232	24.96	81.50	57.55	102.85
233	20.58	92.05	51.57	113.50
301	31.33	66.85	31.33	66.85
302	19.81	81.89	19.81	81.89
310	44.57	44.57	55.98	55.98
311	26.15	63.12	41.17	78.19
312	11.50	78.42	31.43	85.75
313	5.27	89.71	27.35	95.88
320	44.49	44.49	64.09	64.09
321	27.67	61.38	51.66	77.61
322	13.68	75.76	42.63	89.43
323	5.00	86.81	37.59	98.52
331	32.64	61.17	56.59	62.46
332	21.13	73.96	52.23	92.54

213	+ + +	+ + -	+ - +	+ - -
213	0.00	110.95	25.59	117.12
221	36.01	78.75	57.12	94.07
223	11.63	106.75	37.22	118.13
230	60.24	60.24	81.49	81.49
231	43.59	77.46	56.71	95.55
232	30.09	91.90	55.03	108.98
233	21.47	102.71	47.06	118.06
301	40.09	77.33	40.09	77.33
302	25.80	92.67	25.80	92.67
310	55.79	55.79	63.80	63.80
311	37.22	74.40	47.00	81.10
312	22.01	89.73	34.26	95.47
313	11.08	101.04	26.28	106.04
320	55.78	55.73	69.83	69.83
321	38.82	72.68	55.22	84.89
322	24.49	87.08	43.63	97.78
323	13.65	98.14	35.82	107.61
331	42.65	71.97	62.70	89.13
332	30.04	84.94	52.20	99.47

221	+ + +	+ + -	+ - +	+ - -
221	0.00	43.74	73.94	89.95
223	28.42	72.16	67.50	100.98
230	24.59	24.59	92.04	92.04
231	11.50	41.45	65.34	95.57
232	15.12	56.00	80.00	103.47
233	24.35	66.99	76.43	106.60
301	37.74	57.04	37.74	57.04
302	37.53	68.60	37.53	68.60
310	32.41	32.41	58.57	58.57
311	23.21	47.10	52.48	66.24
312	24.76	60.59	50.48	77.29
313	30.89	70.86	51.07	84.37
320	24.28	24.28	71.36	71.36
321	11.31	40.27	65.51	78.64
322	13.58	54.29	62.16	85.49
323	22.53	65.14	60.94	90.92
331	6.69	36.85	76.02	87.19
332	6.28	50.02	72.04	92.47

223	+ + +	+ + -	+ - +	+ - -
223	0.00	100.56	48.56	121.71
230	51.24	51.24	91.41	91.41
231	33.57	69.06	77.61	105.14
232	19.23	83.95	66.50	115.10
233	9.84	95.11	58.76	123.69
301	44.41	78.19	44.41	78.19
302	32.90	92.49	32.90	92.49
310	54.46	54.46	69.15	69.15
311	37.17	72.27	54.31	84.77
312	24.18	87.08	43.48	97.80
313	17.10	96.01	37.10	107.31
320	51.13	51.13	77.29	77.29
321	34.42	67.95	64.20	90.92
322	20.52	82.27	53.92	102.31
323	10.77	93.27	47.00	110.95
331	35.51	65.27	72.61	95.67
332	22.14	78.44	62.98	105.76

230	+ + +	+ + -	+ - +	+ - -
230	0.00	0.00	103.73	103.73
231	18.01	18.01	103.05	103.05
232	33.04	33.04	101.45	101.45
233	44.29	44.29	99.78	99.78
301	54.36	54.36	54.36	54.36
302	59.64	59.64	59.64	59.64
310	36.06	36.06	67.67	67.67
311	40.01	40.01	68.80	68.80
312	47.94	47.94	71.65	71.65
313	55.40	55.40	74.52	74.52
320	22.35	22.35	81.38	81.38
321	27.81	27.81	81.78	81.78
322	37.89	37.89	82.65	82.65
323	47.01	47.01	83.66	83.66
331	18.82	18.82	92.13	92.13
332	30.24	30.24	91.94	91.94

231	+ + +	+ + -	+ - +	+ - -
231	0.00	36.02	96.84	100.66
232	15.02	51.05	91.18	110.47
233	26.28	62.30	86.89	112.18
301	48.97	63.15	48.97	63.15
302	48.63	72.36	48.93	72.36
310	39.76	39.76	68.92	68.82
311	34.18	50.99	63.91	75.91
312	35.89	62.36	61.80	82.74
313	40.53	71.34	61.71	89.07
320	28.41	28.41	81.91	81.91
321	21.33	41.34	76.96	87.36
322	24.25	53.89	73.57	92.27
323	30.98	63.93	71.70	95.96
331	11.46	34.89	87.44	96.62
332	14.66	47.49	83.47	100.26

232	+ + +	+ + -	+ - +	+ - -
232	0.00	66.07	82.51	117.65
233	11.25	77.32	76.22	121.54
301	48.01	72.07	48.01	72.07
302	42.53	83.66	42.53	83.66
310	47.34	47.34	71.43	71.43
311	35.26	62.12	61.56	82.69
312	29.92	75.14	55.31	92.36
313	30.22	84.95	52.28	99.45
320	39.16	39.16	82.78	82.78
321	25.74	54.39	73.77	92.24
322	18.94	67.83	66.96	100.19
323	19.96	78.27	62.55	106.06
331	20.87	49.26	83.70	99.91
332	11.05	62.16	76.77	106.60

233	+ + +	+ + -	+ - +	+ - -
233	0.00	88.57	66.53	127.53
301	49.58	79.29	49.58	79.29
302	40.27	92.26	40.27	92.26
310	54.64	54.64	74.22	74.22
311	39.49	71.05	61.24	88.04
312	29.50	84.91	51.96	99.53
313	25.38	95.19	46.53	107.81
320	48.54	48.54	83.84	83.84
321	33.16	64.58	72.15	95.62
322	21.72	78.41	62.90	105.81
323	16.29	89.06	56.57	113.12
331	30.90	60.19	81.15	101.95
332	18.58	73.20	72.23	110.71

301	+ + +	+ + -	+ - +	+ - -
301	0.00	38.68	0.00	39.58
302	15.78	54.41	15.73	54.41
310	24.79	24.79	24.79	24.79
311	14.95	41.05	14.95	41.05
312	20.33	55.46	20.33	55.46
313	29.14	66.30	29.14	66.30
320	34.88	34.88	34.88	34.88
321	26.11	46.49	28.11	46.49
322	29.15	58.13	29.15	58.13
323	33.99	67.57	33.99	67.57
331	38.70	52.47	38.70	52.47
332	37.78	61.45	37.78	61.45

302	+ + +	+ + -	+ - +	+ - -
302	0.00	70.14	0.00	70.14
310	38.05	38.05	38.05	38.05
311	21.57	55.79	21.57	55.79
312	13.04	70.67	13.04	70.67
313	15.82	81.71	15.82	81.71
320	44.58	44.58	44.58	44.58
321	31.89	59.12	31.89	59.12
322	24.86	72.05	24.86	72.05
323	24.04	82.13	24.04	82.13
331	41.31	62.99	41.31	62.99
332	34.80	73.80	34.80	73.80

31	+ + +	+ + -	+ - +	+ - -
31	0.00	0.00	31.61	31.61
311	18.56	18.66	36.21	36.21
312	34.04	34.04	45.11	45.11
313	45.38	45.38	53.26	53.26
32	13.71	13.71	45.32	45.32
321	21.70	21.70	47.74	47.74
322	34.00	34.00	53.13	53.13
323	44.26	44.26	58.78	58.78
331	28.50	28.50	57.44	57.44
332	36.67	36.67	60.58	60.58

311	+ + +	+ + -	+ - +	+ - -
311	0.00	37.33	29.91	48.54
312	15.38	52.70	32.03	60.69
313	26.71	64.04	37.39	70.18
32	23.01	23.01	48.25	48.23
321	13.16	36.11	43.06	57.07
322	17.77	51.79	42.57	66.32
323	26.52	62.46	44.98	74.04
331	23.75	41.42	53.56	64.71
332	24.37	52.49	51.95	71.67

312	+ + +	+ + -	+ - +	+ - -
312	0.00	66.08	26.09	74.25
313	11.34	79.42	26.50	84.42
32	36.39	36.39	54.36	54.36
321	21.02	52.67	43.88	66.41
322	11.82	66.72	37.80	75.15
323	13.66	77.57	36.12	87.05
331	29.20	54.30	53.90	72.46
332	21.76	66.39	47.94	81.78

313	+ + +	+ + -	+ - +	+ - -
313	0.00	90.75	22.05	94.96
32	46.97	46.97	60.40	60.40
321	30.62	63.60	47.13	74.67
322	17.56	77.80	37.58	87.11
323	10.27	88.73	32.33	96.70
331	36.75	64.32	55.80	78.81
332	25.94	76.94	47.09	89.47

32	+ + +	+ + -	+ - +	+ - -
32	0.00	0.00	59.03	59.03
321	16.99	16.99	60.52	60.52
322	31.42	31.42	63.95	63.95
323	42.50	42.50	67.70	67.70
331	18.41	18.41	70.56	70.56
332	30.00	30.00	72.32	72.32

321	+ + +	+ + -	+ - +	+ - -
321	0.00	33.97	55.22	67.34
322	14.44	48.41	55.09	74.47
323	25.52	59.49	55.93	80.48
331	10.59	33.70	66.81	75.95
332	14.97	46.34	64.64	81.22

322	+ + +	+ + -	+ - +	+ - -
322	0.00	62.65	49.72	84.09
323	11.08	73.93	47.47	91.63
331	19.19	47.55	65.25	81.42
332	9.94	60.46	59.66	89.25

323	+ + +	+ + -	+ - +	+ - -
323	0.00	89.01	42.56	100.1
331	29.05	58.34	65.17	85.95
332	16.82	71.36	57.13	95.44

331	+ + +	+ + -	+ - +	+ - -
331	0.00	29.96	77.41	85.19
332	13.17	43.13	74.93	89.32

332	+ + +	+ + -	+ - +	+ - -
332	0.00	56.31	69.50	95.55

APPENDIX C

Computer Program to get the Crystallographic Data of Ni_3Sn Martensite

```
      PROGRAM TEM(INPUT,OUTPUT,TAPE10=INPUT,TAPE20=OUTPUT)
      INTEGER HKL(3,50 ),P(3,11)
      DIMENSION A(50 ,13),PA(5,6)
      DATA PA/47.,63.5,87.,66.5,70.,47.,10.5,45.,86.,23.,63.5,16.5,28.5,
     *49.5,7.,67.,45.,28.5,29.5,22.7,66.5,66.,49.5,20.5,43.,70.,25.,7.,
     *24.7,43./
      DATA P/2,1,-2,2,-2,1,1,2,-2,1,-2,2,2,-1,2,-2,1,2,-2,2,1,2,2,-1,-1,
     *2,2,2,1,2,2,2,1/
      LP=4
      II=1
      JJ=2
      KK=2
      Q=1.5
      WRITE(20,11) II,JJ,KK
11    FORMAT(////,10X,"PICTURE     B",//,10X,"REFERENCE   ",3I2)
      DO 2000 MA=1,LP
      INDEX=1
      DO 1000I=1,20
      DO 1000 J=1,20
      DO1000 K=1,20
      IF(K.LT.J.OR.J.LT.I)GO TO 1001
      IF(I.EQ.J.AND.I.EQ.K.AND.I.NE.1)GO TO 1001
      THETA=ACOS(K/FLOAT(I*I+J*J+K*K)**.5)*57.29
      IF(THETA.GT.45..OR.THETA.LT.0.) GO TO 1001
      PHI=ACOS(-I/FLOAT(I*I+J*J)**.5)*57.2957
      IF(PHI.LT.90.OR.PHI.GT.126.)GO TO 1001
      A(INDEX,1)=THETA
      A(INDEX,2)=PHI-90.
      HKL(1,INDEX)=-I
      HKL(2,INDEX)=J
      HKL(3,INDEX)=K
      DO 100 LL=3,13
      L=LL-2
      CH1=((KK*J-JJ*K)*(KK*J-JJ*K)*(KK*I+II*K)*(KK*I+II*K)*(JJ*I+II*J)*(
     *JJ*I+II*J))
      CH2=((P(3,L)*J-P(2,L)*K)*(P(3,L)*J-P(2,L)*K)*(P(3,L)*I+P(1,L)*K)*(
     *P(3,L)*I+P(1,L)*K)*(P(2,L)*I+P(1,L)*J)*(P(2,L)*I+P(1,L)*J))
      CH3=(KK*J-JJ*K)*(P(3,L)*J-P(2,L)*K)*(KK*I+II*K)*(P(3,L)*I+P(1,L)*K
     *)*(JJ*I+II*J)*(P(2,L)*I+P(1,L)*J)
      AAA=ABS(CH3)/(CH2*CH1)**.5
      IF(AAA.GE.1.)AAA=1.
100   A(INDEX,LL)=ACOS(AAA)*57.29578
      LPP=LP-1
      DO 500 LPL=1,LPP
      DO 600 LL=3,13
      IF(A(INDEX,LL).GE.PA(LPL,MA)-Q .AND.A(INDEX,LL).LE.PA(LPL,MA)+Q )
     *GO TO 111
600   CONTINUE
      GO TO 1001
111   CONTINUE
500   CONTINUE
      INDEX=INDEX+1
1001  CONTINUE
1000  CONTINUE
      WRITE(20,12)MA
12    FORMAT(//,10X,"LINE        ",I2)
      WRITE(20,1)
1     FORMAT(//,5X,"HKL",7X,"THETA",5X,"PHI",3X,"2 1-2",3X,"2-2 1",3X,"1
     * 2-2",3X,"1-2 2",3X,"2-1 2",2X,"-2 1 2",2X,"-2 2 1",3X,"2 2-1",2X,
     *"-1 2 2",3X,"2 1 2",3X,"2 2 1",2X,"REF 122"//)
      IN=INDEX-1
      DO 300 J=1,IN
      WRITE(20,2) (HKL(K,J),K=1,3),(A(J,L),L=1,13)
2     FORMAT(3I4,13F8.2)
300   CONTINUE
2000  CONTINUE
      STOP
      END
```